



1                   **A multi-model comparison of meteorological drivers of surface ozone over**  
2                   **Europe**

3  
4 Noelia Otero<sup>1,3</sup>, Jana Sillmann<sup>2</sup>, Kathleen A. Mar<sup>1</sup>, Henning W. Rust<sup>3</sup>, Sverre Solberg<sup>4</sup>,  
5 Camilla Andersson<sup>5</sup>, Magnuz Engardt<sup>5</sup>, Robert Bergström<sup>5</sup>, Bertrand Bessagnet<sup>6</sup>,  
6 Augustin Colette<sup>6</sup>, Florian Couvidat<sup>6</sup>, Cornelius Cuvelier<sup>7</sup>, Svetlana Tsyro<sup>8</sup>, Hilde  
7 Fagerli<sup>8</sup>, Martijn Schaap<sup>9,3</sup>, Astrid Manders<sup>9</sup>, Mihaela Mircea<sup>10</sup>, Gino Briganti<sup>10</sup>, Andrea  
8 Cappelletti<sup>10</sup>, Mario Adani<sup>10</sup>, Massimo D'Isidoro<sup>10</sup>, María-Teresa Pay<sup>11</sup>, Mark  
9 Theobald<sup>12</sup>, Marta G. Vivanco<sup>12</sup>, Peter Wind<sup>8,13</sup>, Narendra Ojha<sup>14</sup>, Valentin Raffort<sup>15</sup>  
10 and Tim Butler<sup>1,3</sup>

11  
12 <sup>1</sup>Institute for Advanced Sustainability Studies e.V., Potsdam, Germany

13 <sup>2</sup>CICERO Center for International Climate Research, Oslo, Norway

14 <sup>3</sup>Freie Universität Berlin, Institut für Meteorologie, Berlin, Germany

15 <sup>4</sup>Norwegian Institute for Air Research (NILU), Box 100, 2027 Kjeller, Norway

16 <sup>5</sup>SMHI, Swedish Meteorological and Hydrological Institute Norrköping, Norrköping,  
17 Sweden

18 <sup>6</sup>INERIS, Institut National de l'Environnement Industriel et des Risques, Verneuil en  
19 Halatte, France

20 <sup>7</sup>European Commission, Joint Research Centre (JRC), Ispra, Italy

21 <sup>8</sup>MET Norway, Norwegian Meteorological Institute, Oslo, Norway

22 <sup>9</sup>TNO, Netherlands Institute for Applied Scientific Research, Utrecht, the Netherlands

23 <sup>10</sup>ENE-National Agency for New Technologies, Energy and Sustainable Economic  
24 Development, Bologna, Italy

25 <sup>11</sup>Barcelona Supercomputing Center, Centro Nacional de Supercomputación, Jordi  
26 Girona, 29, 08034 Barcelona, Spain

27 <sup>12</sup>CIEMAT, Atmospheric Pollution Unit, Avda. Complutense, 22, 28040 Madrid, Spain

28 <sup>13</sup>Faculty of Science and Technology, University of Tromsø, Tromsø, Norway

29 <sup>14</sup>Max-Planck-Institut für Chemie, Mainz, Germany

30 <sup>15</sup>CEREA, Joint Laboratory Ecole des Ponts ParisTech – EDF R&D, Champs-Sur-  
31 Marne, France

32

33

34

35

36 **Abstract.** The implementation of European emission abatement strategies has led to  
37 significant reduction in the emission of ozone precursors during the last decade. Ground  
38 level ozone is also influenced by meteorological factors such as temperature, which  
39 exhibit interannual variability, and are expected to change in the future. The impacts of  
40 climate change on air quality are usually investigated through air quality models that  
41 simulate interactions between emissions, meteorology and chemistry. Within a multi-  
42 model assessment, this study aims to better understand how air quality models represent  
43 the relationship between meteorological variables and surface ozone concentrations  
44 over Europe. A multiple linear regression (MLR) approach is applied to observed and  
45 modelled time series across ten European regions in springtime and summertime for the  
46 period of 2000–2010 for both models and observations. Overall, the air quality models  
47 are in better agreement with observations in summertime than in springtime, and  
48 particularly in certain regions, such as France, Mid-Europe or East-Europe, where local  
49 meteorological variables show a strong influence on surface ozone concentrations.



50 Larger discrepancies are found for the southern regions, such as the Balkans, the Iberian  
51 Peninsula and the Mediterranean basin, especially in springtime. We show that the air  
52 quality models do not properly reproduce the sensitivity of surface ozone to some of the  
53 main meteorological drivers, such as maximum temperature, relative humidity and  
54 surface solar radiation. Specifically, all air quality models show more limitations to  
55 capture the strength of the relationship ozone-relative humidity detected in the observed  
56 time series in most of the regions, in both seasons. Here, we speculate that dry  
57 deposition schemes in the air quality models might play an essential role to capture this  
58 relationship. We further quantify the relationship between ozone and maximum  
59 temperature ( $m_{O_3-T}$ , climate penalty) in observations and air quality models. In  
60 summertime, most of the air quality models are able to reproduce reasonably well the  
61 observed climate penalty in certain regions such as France, Mid-Europe and North Italy.  
62 However, larger discrepancies are found in springtime, where air quality models tend to  
63 overestimate the magnitude of observed climate penalty.

64  
65  
66  
67  
68  
69  
70  
71  
72  
73

## 74 1. Introduction

75  
76  
77  
78  
79  
80  
81  
82  
83  
84  
85  
86  
87  
88  
89

Tropospheric ozone is recognised as a threat to human health and ecosystem productivity (Mills et al. 2007). Moreover, ozone is an important greenhouse gas (IPCC, 2013). It is produced by photochemical oxidation of carbon monoxide and volatile organic compounds (VOCs) in the presence of nitrogen oxides ( $NO_x=NO+NO_2$ ) (Jacob and Winner, 2009). While it is an important pollutant on a regional scale, due to the long-range transport effect it may also influence air quality on a hemispheric scale (Monks et al., 2015, Hedegaard et al, 2013). Moreover, its strong relationship with temperature represents a major concern, since under a changing climate the efforts on new air pollution mitigation strategies might be insufficient. This effect, referred as climate penalty (Wu et al., 2008), is expected to play an important role on future air quality (Hendriks et al. 2016). Therefore it is essential to better understand the potential implications of climate change on pollutant levels. In a comprehensive review of the existing literature about the robustness of climate penalty on Europe, Colette et al. (2015) concluded that the climate change might act against mitigation measures.

90  
91  
92  
93  
94  
95  
96  
97  
98  
99

Previous studies have shown that the reduction of emissions of ozone precursors,  $NO_x$  and VOCs, lead to a decrease in tropospheric ozone concentrations in Europe (Solberg et al. 2005, Jonson et al. 2006). However, there is also a large year-to-year variability due to weather conditions (Andersson et al. 2007). There is a strong correlation between ozone and temperature that has been associated with the temperature-dependent lifetime of peroxyacetyl nitrate (PAN), and also due to the temperature dependence of biogenic emission of isoprene (Sillman and Samson, 1995). Substantial increases in surface ozone have been associated with high temperatures and stable anticyclonic, sunny conditions that promote ozone formation (Solberg et al. 2008). Ozone peak



100 concentrations are also affected by closing of the plants' stomata at very high  
101 temperatures (Hodnebrog et al. 2012). Several studies have assessed the model  
102 dependence of ozone on temperature (e.g. Steiner et al. 2006, Rasmussen et al. 2013).  
103 Recently, Coates et al. (2016) used a box model to investigate the influence of  
104 temperature and NO<sub>x</sub> on ozone production. Their analysis suggested that reductions in  
105 NO<sub>x</sub> would be required to offset additional ozone increase due to increasing  
106 temperatures under a warmer climate. An extensive review about the impacts of  
107 temperature on ozone production can be found in Pusede et al. (2015).

108

109 Previous studies have shown the importance of relative humidity on ozone pollution  
110 episodes (Camalier et al. 2007, Davies et al. 2011). Regional studies reported a negative  
111 relationship between ozone and relative humidity (Dueñas et al. 2002, Elminir 2005,  
112 Demuzere et al., 2009). Some authors attributed this negative correlation to the  
113 photolysis of ozone and subsequent loss of O<sub>1</sub>(D) to H<sub>2</sub>O (Jacob and Winner). High  
114 levels of humidity are usually related with enhanced cloud cover and thus reduced  
115 photochemistry (Dueñas et al. 2002, Camalier et al. 2007). Andersson and Engardt  
116 (2010) highlighted the importance of including meteorological dependence for dry  
117 deposition of ozone to vegetation, also incorporating soil moisture dependence. With a  
118 simple modelling approach, Kavassalis and Murphy (2017) found that the relationship  
119 ozone-relative humidity was well captured by the inclusion of the vapour pressure  
120 deficit-dependent dry deposition, indicating the relevance of detailed dry deposition  
121 schemes in the CTMs.

122 Increasing solar radiation leads to an increase of ozone, though with a weak effect  
123 (Dawson et al. 2007) and it has been suggested that it could reflect in part the  
124 association of clear sky with high temperatures (Ordóñez et al., 2005). Then, changes in  
125 cloud cover can also affect the photochemistry of ozone production and loss (Jacob and  
126 Winner, 2009). Additionally, low wind speed is usually associated with high ozone  
127 pollution levels (Jacob and Winner, 2009).

128 The influence of climate change on ozone and its precursors can involve multiple  
129 processes (Colette et al, 2015). A common approach to study the impact of climate  
130 change on air quality requires the use of air quality models that aim to represent  
131 dynamic and chemical processes in the atmosphere. The relevance of climate change for  
132 future European air quality has been assessed in several studies that also reflect  
133 differences depending on the modelling system and future emissions scenarios adopted  
134 for each study (e.g. Lagner et al. 2005, Meleux et al. 2007, Anderson and Engardt,  
135 2010).

136

137 Air quality models can be divided into two categories: offline chemistry transport  
138 models (CTMs) in which the model chemistry runs using meteorological data as input,  
139 and online models that allow coupling and integration of chemistry with some of the  
140 physical components to various degrees (Baklanov et al. 2014). Differences between  
141 offline and online modelling approaches can be fairly small or significant, depending on  
142 the level of the model complexity and simulated variables (Zhang, 2008). The large  
143 number and complex interactions between meteorology and chemistry in the  
144 atmosphere influence the ability of the model to represent observed situations (Kong et  
145 al. 2014). Due to assumptions, parametrizations and simplifications of processes, the  
146 models themselves are subject to large uncertainties (Manders et al. 2012), which have  
147 been reflected in some regional differences in the magnitude of surface ozone response



148 to projected climate change (Andersson and Engardt, 2010). Thus, model biases when  
149 compared to observations still remain a concern, especially in terms of the response of  
150 air quality under future climate (Fiore et al. 2009, Rasmussen et al. 2012). Comparisons  
151 between model outputs and measurements of available observational dataset assess the  
152 reliability of air quality models, and they are essential to quantify the models ability to  
153 reproduce observations.

154  
155 The EURODELTA project was initiated by the Task Force on Measurement and  
156 Modelling and the Joint Research Centre of the European Commission to provide a  
157 benchmark for the EMEP model in order to assess its relevance for policy support  
158 (Colette et al. 2017a). These multi-model exercises contribute to further improving  
159 modelling techniques and understanding the associated uncertainties in the models  
160 performance. Previous exercises have evaluated the performance of chemistry transport  
161 models for future European air quality (e.g. van Lon et al. 2007, Thunis et al. 2008).  
162 Recently, Bessagnet et al. (2016) presented an intercomparison and evaluation of  
163 chemistry transport model performance with a joint analysis of some meteorological  
164 fields. They highlighted the limitations of models to simulate meteorological variables,  
165 such as wind speed and planetary boundary layer height. Particularly, in the case of  
166 ozone, they showed the importance of boundary conditions on model calculations.  
167 Within this framework, the ongoing Eurodelta-Trends (EDT) exercise (Colette et al.  
168 2017a) builds upon this tradition and focuses on the context of air quality trends  
169 modelling. This exercise has been designed to better understand the evolution of air  
170 pollution and its drivers over the last two decades (1990-2010) by the use of state-of-  
171 the-art air quality models. The EDT project will allow the evaluation of the skill of  
172 regional air quality models and quantification of the role of the different key driving  
173 factors of surface ozone, such as emissions changes, long-range transport and  
174 meteorological variability. One of the main goals of the EDT project is to assess the  
175 efficiency of mitigation strategies for improving air quality (more details can be found  
176 in Colette et al. 2017a).

177  
178 Quantification and isolation of the effects of meteorology on ozone is a challenge, due  
179 to the complex interrelation between ozone, meteorology, emissions and chemistry  
180 (Solberg et al. 2015). There is a large number of representative studies in the literature  
181 that have established the relationship between surface ozone concentrations and  
182 meteorological variables using statistical modelling techniques (e.g. Bloomfield et al.  
183 1996, Chaloukai et al. 2003, Barrero et al. 2005, Ordóñez et al., 2005, Camalier et al.,  
184 2007, Seo et al., 2014, Porter et al. 2015, Otero et al., 2016). Most of these works  
185 examined the impact of meteorology on ozone pollution levels through observational  
186 datasets. Only a few studies, to our knowledge, examined the statistical relationship  
187 between surface ozone and meteorological parameters from models.

188  
189 Davis et al. (2011) developed regression models to analyse the observed and modelled  
190 relationship between meteorology and surface ozone across the Eastern of U.S. They  
191 found that the Community Multiscale Air Quality (CMAQ) model did not capture the  
192 effect of temperature and relative humidity on daily maximum 8-h ozone and it  
193 generally underestimated the observed sensitivities to both meteorological variables,  
194 especially in the northeast. Rasmussen et al. (2012) examined the ozone-temperature  
195 relationship in a coupled chemistry-climate model and they found that the model  
196 underestimated the effect of temperature on ozone over the Mid-Atlantic. Lemaire et al.  
197 (2016) proposed a combined statistical and deterministic approach to assess the air



198 quality response to projected climate change. Based on a data set from a deterministic  
199 climate and chemistry models, they identified the two major drivers of surface ozone  
200 over eight European regions, selected from a set of potential predictors that reached the  
201 highest correlations with ozone. Afterwards they built statistical models consisting of  
202 generalized linear models, which could be used to predict air quality.

203  
204 Given that meteorology plays an essential role for surface ozone concentrations, it  
205 might be a considerable source of uncertainties in model outputs. The present study,  
206 thus, aims to provide a simple method to examine the influence of meteorological  
207 variability on modelled surface ozone concentrations over Europe. Specifically, our  
208 analysis focuses on the ozone season (April to September) over the years 2000-2010.  
209 The choice of this period is mainly motivated by the availability of the observational  
210 dataset from Schnell et al. (2014, 2015) (see section 2.1). Within the EDT framework, a  
211 recent report has presented the main findings on the long-term evolution of air quality  
212 (Colette et al. 2017b). Part of these results was obtained from the analysis of the 1990s  
213 (1990-2000) and 2000s (2000-2010) separately. Consistently, we decided to focus on  
214 the second decade, for which the interpolated dataset of observed on maximum daily 8-  
215 hourly mean ozone (MDA8 O<sub>3</sub>) used in this study was available. Similarly to Otero et  
216 al. (2016), we apply a multiple linear regression approach to examine the  
217 meteorological influence MDA8 O<sub>3</sub>. Statistical models are developed separately for  
218 observational datasets and air quality models, with the primary focus on examining the  
219 relationship between MDA8 O<sub>3</sub> and potential meteorological drivers in the air quality  
220 models and comparing these with the corresponding relationships determined from  
221 observed data. Therefore, this study offers a method of model evaluation capable of  
222 understanding the discrepancies between air quality models and observations in terms of  
223 representing the relationship to meteorological input variability.

224  
225 The present paper is structured as follows. Section 2 describes the observational data as  
226 well as the air quality models studied here. The methodology and the design of the  
227 statistical models are introduced in section 3. Section 4 discusses the results and the  
228 summary and conclusions are discussed in section 5.

## 229 **2. Data**

### 230 **2.1. Observations**

231  
232 This study uses gridded MDA8 O<sub>3</sub> concentrations created with an objective-mapping  
233 algorithm developed by Schnell et al. (2014). They applied a new interpolation  
234 technique over hourly observations of stations from the European Monitoring and  
235 Evaluation Programme (EMEP) and the European Environment Agency's air quality  
236 database (AirBase) to calculate surface ozone averaged over 1° by 1° grid cells.  
237 Recently, Otero et al. (2016) used this dataset for examining the influence of synoptic  
238 and local meteorological conditions over Europe. This interpolated product offers a  
239 possibility to establish a direct comparison between observations and CTMs. However,  
240 it must be acknowledged that for some areas with a low number of stations (i.e. the  
241 southeastern or northeastern European regions) the values interpolated into the 1x1  
242 degree grid cells may not be representative of such large scales. A complete description  
243 of this process can be found in Schnell et al. (2014, 2015). The gridded dataset covers a  
244 total of 15-years (1998-2012), but here we use a common period of 11-years for both  
245 observations and CTMs (2000-2010).  
246  
247



248

249 This study investigates the observed influence of meteorological variables on MDA8  
250 O<sub>3</sub>, based on the ERA-Interim reanalysis product provided by the European Centre for  
251 Medium-Range Weather Forecasts (ECMWF) at 1°x1° resolution (Dee et al. 2011).  
252 Meteorological reanalyses products are essentially model simulations constrained by  
253 observations and they have been widely validated against independent observations.  
254 Daily mean values are calculated as the mean of the four available time steps at 00, 06,  
255 12, and 18UTC for 10m wind speed components (u and v) and 2m relative humidity.  
256 Maximum temperature is approximated by the daily maximum of those time steps,  
257 while daily mean surface solar radiation is obtained from the 3-hourly values provided  
258 for the forecast fields.

259

## 260 2.2. Chemistry Transport Models (CTMs)

261

262 A set of state-of-the-art air quality models participating in the EDT exercise is used  
263 here: LOTOS-EUROS (Schaap et al., 2008, Manders et al. 2017), EMEP/MSC-W  
264 (Simpson et al., 2012), CHIMERE (Mailer et al., 2017), MATCH (Robertson et al.,  
265 1999), MINNI (Mircea et al., 2016) and WRF-Chem (Grell et al. 2005, Mar et al. 2016).  
266 The domain of the CTMs extends from 17°W to 39.8°E and from 32°N to 70°N and it  
267 follows a regular latitude-longitude projection of 0.25x0.4 respectively. The main  
268 features of the CTM setup are largely constrained by the EDT experimental protocol  
269 (e.g. meteorology, boundary conditions, emissions, resolution, see Colette et al. 2017a  
270 for further details). For instance, the boundary conditions were defined from  
271 climatology of observational data for most of the experiments of the EDT exercise  
272 (included the data used here). However, the representation of physical and chemical  
273 processes and the vertical distribution differ in the CTMs, as well as the vertical  
274 distribution of model layers (including altitude of the top layer and derivation of surface  
275 concentration at 3m height in the case of EMEP, LOTOS-EUROS and MATCH).  
276 Moreover, there were no specific constraints imposed on biogenic emissions (including  
277 soil NO emissions), which are represented by most of the models using an online  
278 module (Colette et al. 2017a). Since we aim here to compare the modelled relationship  
279 between meteorology and surface ozone, prescribing common features in the CTMs is  
280 particularly an advantage to identify potential sources of discrepancies.

281

282 Only one of the participating CTMs included online coupled chemistry/meteorology  
283 (WRF-Chem), while all the rest of the models used are offline. The CTMs were forced  
284 by regional climate model simulations using boundary conditions from the ERA-Interim  
285 global reanalysis (Dee et al., 2011). Most of these offline CTMs used the same  
286 meteorological input data, with a few exceptions. Three of them (EMEP, CHIMERE  
287 and MINNI) used input meteorology from the Weather Research and Forecast Model  
288 (WRF) (Skamarock et al. 2008). LOTOS-EUROS and MATCH used the input  
289 meteorology produced by RACMO2 (van Meijgaard, 2012) and HIRLAM (Dahlgren et  
290 al. 2016), respectively. Unlike the rest of the regional climate models, RACMO2 used  
291 in the EDT exercise excluded nudging towards ERA-Interim, which might have some  
292 impact in the meteorological fields generated by RACMO2. As mentioned, WRF-Chem  
293 couples the meteorology simulations online with chemistry. The meteorology used to  
294 drive WRF-Chem (initial and lateral boundary conditions and the application of limited  
295 four-dimensional data assimilation; see Colette et al GMD 2017a) is the same WRF  
296 meteorology from Skamarock et al. (2008) used as input for the EMEP, CHIMERE, and  
297 MINNI runs. Table 1 summarises the CTMs and the corresponding sources of



298 meteorological input data used here. It is important to highlight that though WRF-Chem  
299 is not strictly a CTM, in order to avoid confusion with the statistical models developed  
300 in this study, we refer to all the air quality models considered (offline and online  
301 models) as CTMs hereafter. As with the observations, CTMs and their meteorological  
302 counterpart were interpolated to a common grid with  $1^\circ \times 1^\circ$  horizontal resolution. The  
303 use of a coarser resolution could have an impact in some regions with a complex  
304 orography where airflow is usually controlled by mesoscale phenomena (e.g. see-breeze  
305 and mountain-valley winds) or in regions characterized by high emissions densities  
306 (Schaap et al., 2015, Gan et al. 2016 ). In such cases the use of a finer grid could be  
307 beneficial to capture the variability of local processes.

308

309 A set of meteorological parameters was selected from the meteorological input data for  
310 the regression analyses. Similarly to the procedure with ERA-Interim, daily means are  
311 obtained from the available time steps every 3 hours in the case of WRF and RACMO2,  
312 and every 6 hours for HIRLAM for the following variables: 10m wind speed  
313 components, 2m relative humidity and surface solar radiation. Maximum temperature is  
314 also approximated by the daily maximum of those time steps.

315

### 316 3. Multiple Linear regression model

317

318 Summertime usually brings favourable conditions for high tropospheric ozone  
319 concentrations, such as air stagnation due to high-pressure systems, warmer  
320 temperatures, higher UV radiation, and lower cloud cover (Dawson et al. 2007). As  
321 stated above, the impact of meteorology on ozone concentration has been addressed  
322 through a wide variety of statistical methods in the literature. This study attempts to  
323 better understand how CTMs represent the influence of meteorology on ozone. To this  
324 aim, we use a multiple linear regression approach that can provide useful information of  
325 sensitivities in the distribution of ozone concentration as a whole (Porter et al., 2015).

326

327 A total of five meteorological predictors (Table 2) are selected based on the existing  
328 literature that has shown their strong influence on ozone pollution. (e.g. Bloomfield et  
329 al. 1996, Barrero et al. 2005, Camalier et al. 2007, Dawson et al. 2007, Rasmussen et al.  
330 2012, Davis et al. 2011, Doherty et al., 2013, Otero et al. 2016). Moreover, it has been  
331 shown that the occurrence of air pollution episodes might increase when the pollution  
332 levels of the previous day are higher than normal (Ziomas et al. 1995). Then, apart from  
333 the meteorological predictors, we add the effect of the lag of ozone (MDA8 from the  
334 previous day) in order to examine the role of ozone persistence. Additionally, we  
335 include harmonic functions that capture the effect of seasonality as in Rust et al. al  
336 (2009) and Otero et al. (2016), which is referred as “day” in the MLRs (see Table 2).

337

338 For this study, we divide the European domain into 10 regions: England (EN), Inflow  
339 (IN), Iberian Peninsula (IP), France (FR), Mid-Europe (ME), Scandinavia (SC), North  
340 Italy (NI), Mediterranean (MD), Balkans (BA) and Eastern Europe (EA). These regions  
341 are based on those defined in the recent ETC/ACM Technical Paper (Colette et al.  
342 2017b). For our study, we further subdivide the original Mediterranean region (MD)  
343 into a region covering the Balkans (BA), due to the strong influence of the ozone  
344 persistence on MDA8 O<sub>3</sub> over this particular region as noted previously in Otero et al.  
345 (2016). Figure 1 shows the spatial coverage of each region and Table 3 lists their  
346 coordinates. As shown Otero et al. (2016), the relative importance of predictors in the  
347 MLRs shows distinct seasonal patterns. Then, multiple linear regression models (MLR,



348 hereafter) are developed for each region for two seasons: springtime (April-May-June,  
349 AMJ) and summertime (July-August-September, JAS). These seasons differ from the  
350 meteorological definition, but cover the period when surface ozone typically reaches its  
351 highest concentrations (i.e. April-September). Since the observations did not cover  
352 exactly the whole European domain as CTMs, we applied an observational-mask to use  
353 the same number of grid-cells for CTMs and observations. Data used to estimate  
354 parameters of the MLR were spatially averaged over each region. Thus, we compare  
355 MLRs developed separately for CTMs and observations at each region and season. The  
356 observational dataset contains the gridded MDA8O3 and the meteorology input from  
357 ERA-Interim, while the dataset for the CTMs contains the MDA8O3 from each one of  
358 them along with the corresponding meteorological input (e.g. LOTOS and RACMO2,  
359 CHIMERE and WRF) (see table 1).

360

361 A MLR is built to describe the relationship between MDA8 O3 (predictand) and a set of  
362 covariates (or predictors) describing seasonality, ozone persistence and the influence of  
363 meteorological fields (table 2). A data series  $y_t$ ,  $t=1,\dots,N$  (e.g. observations or CTM  
364 simulations) for a given region and season is conceived as a Gaussian random variable  
365  $Y_t$  with varying mean  $\mu_t$  and homogeneous variance  $\sigma^2$ . The mean  $\mu_t$  is described as a  
366 linear function of the covariates, i.e.

367

$$368 Y_t \sim \mathcal{N}(\mu_t, \sigma^2),$$

$$369 \mu_t = \beta_0 + \beta_{\sin} \sin\left(\frac{2\pi}{365.25} d_t\right) + \beta_{\cos} \cos\left(\frac{2\pi}{365.25} d_t\right) + \beta_{lag} y_{t-1} + \sum_{k=1}^K \beta_k x_{t,k} \quad (1)$$

370

371 with  $t$  indexing daily values and  $d_t$  referring to the day in the year associated with the  
372 index  $t$ .  $\beta_0$  is a constant offset,  $\beta_{\sin}$  and  $\beta_{\cos}$  are the first order coefficient of a Fourier  
373 series (e.g. Rust et al. 2009, 2013, Fischer et al. 2017),  $\beta_{lag}$  describes the persistence  
374 with respect to the previous day concentration  $y_{t-1}$ ; if  $t$  is the first day in the late  
375 summer season (JAS, July 1<sup>st</sup>),  $y_{t-1}$  is the concentration of June 30<sup>th</sup>. Further regression  
376 coefficients  $\beta_k$  describe the linear relation to potential meteorological drivers (see table  
377 2). For covariates standardized to unit variance, the regression coefficients ( $\beta$ ) are  
378 standardised coefficients giving the change in the predictand with the covariate in units  
379 of covariate standard deviation.

380

381 Following the same strategy as used in Otero et al. (2016), the MLRs are developed  
382 through several common steps: 1) starting with the full set of potentially useful  
383 components in the predictor, a stepwise backward regression using the Akaike  
384 Information Criterion (AIC) as a selection criterion removes successively those  
385 components in the predictor, which contribute least to the model performance; and 2) a  
386 multi-collinearity index known as variance inflation factor (VIF, Maindonald and Braun  
387 2006) is used to detect multi-collinearity problems in the predictor (i.e. high correlations  
388 between two or more components in the predictor). Components with a VIF above 10  
389 are left out of the predictor (Kutner et al 2004).

390

391 The statistical performance of each MLR (built separately from observations and  
392 CTMs) is assessed through the adjusted coefficient ( $R^2$ ) and the root mean square error  
393 (RMSE). The  $R^2$  estimates the fraction of total variability described by the MLR and the  
394 RMSE gives the average deviation between model and observation obtained in the  
395 MLR. We also examine the relative importance of the individual components in the  
396 predictor. According to the method proposed by Lindeman et al (1980), the relative





397 importance of each predictor is estimated by its contribution to the  $R^2$  coefficient  
398 (Grömping 2007). We assess the sensitivities of ozone to the predictors through the  
399 standardised coefficients obtained from the regression. These coefficients indicate the  
400 changes in the ozone response to the changes in the predictors, in terms of standard  
401 deviation. Thus, for every standard deviation unit increase (decrease) of a specific  
402 predictor, the predictand (MDA8 O<sub>3</sub>) will increase (decrease) the amount indicated by  
403 its coefficient in standard deviation units,. The use of standardised coefficients allows  
404 us to establish a direct comparison in the influence of individual predictors. The effect  
405 of seasonality introduced by the harmonic functions (namely, “day”, table 2) is kept in  
406 the MLRs (Eq. 1) for its usefulness in improving the power of the regression analysis,  
407 however further explanation about the effect of the predictors focuses on the rest of the  
408 variables.

409

## 410 4. Results and discussion

411

### 412 4.1. CTM performance by region

413

414 We compare the seasonal cycle of observations and CTMs through the time series of  
415 daily averaged values of MDAO8 O<sub>3</sub> from observations and CTMs for the whole period  
416 (i.e. April-September, 2000-2010) spatially averaged over each region. Furthermore,  
417 correlation coefficients between both CTMs and observations at each region and season  
418 are used to quantify the CTM performance.

419

#### 420 4.1.1. Seasonal cycle of MDA8 O<sub>3</sub>

421

422 We examine the ozone seasonal cycle represented by both the observational and  
423 modelled dataset. Figure 2 depicts daily averages during 2000-2010 of MDA8 O<sub>3</sub> at  
424 each region for the CTMs and observations. In general, all CTMs are biased high  
425 compared with observations. CTM results are visually closer to observations in the  
426 northwestern regions (i.e. IN, EN and FR), while the spread becomes larger over the  
427 southern and southeastern regions (i.e. BA, NI, MD). The IN, EN and SC regions show  
428 the highest observed concentrations in the starting months (AMJ), which is not  
429 generally well captured by most of the CTMs, and they show a more flat timeline (e.g.  
430 LOTOS, MATCH, CHIMERE or WRF-Chem). For example, in the SC region, some of  
431 the CTMs underestimate the ozone concentrations in AMJ (i.e. WRF-Chem, CHIMERE  
432 and MINNI). The rest of the regions show the highest observed concentrations in JAS,  
433 which is generally overestimated by the CTMs. Models show discrepancies when  
434 compared to each other and to observations, and in some regions we find substantial  
435 differences. Larger discrepancies are found in the southern regions, such as IP, MD and  
436 BA, where the models show a considerable spread. There, the CTMs are not able to  
437 capture the variability of MDA8 O<sub>3</sub> and they exhibit a different behaviour when  
438 compared to each other. For instance, the EMEP model shows a peak of ozone levels in  
439 April, while CHIMERE and MINNI show a peak in July. Overall LOTOS shows a  
440 relatively constant positive bias in all regions, more evident in the MD and NI regions.  
441 WRF-Chem tends to underestimate the ozone concentrations at the start of the seasonal  
442 period in some regions (e.g. SC, ME, EN, or EA).

443

444 CTM assessments have been presented in early EURODELTA exercises, although with  
445 a different set up for different purposes, which makes it difficult to establish a direct  
446 comparison on the performance of the models. For instance, Colette et al. (2017b)



447 reported systematic differences among some models (i.e. CHIMERE, EMEP and  
448 LOTOS) when examining the long-term mean ozone concentration during the whole  
449 period of 1990-2010. Bessagnet et al. (2016) showed that most of the models in their  
450 study, (e.g. CHIMERE, LOTOS, or MINNI among others) overestimated the ozone  
451 concentrations in the selected study period. Specifically, they found a larger spread  
452 during nighttime than daytime, which was suggested to be related to the vertical mixing,  
453 given that most of the models shared the same meteorology but different vertical  
454 resolution and boundary conditions.

455

456 4.1.2. Correlation coefficients between modelled and observed time series

457

458 The correlation coefficients between the observed and modelled values of MDA8 O<sub>3</sub> at  
459 each region and in each season are shown in Fig. 3. Overall, MDA8 O<sub>3</sub> from the CTMs  
460 is better correlated with observations in JAS than in AMJ in the regions ME, NI, EA  
461 and EN. As expected from inspection of the average time series (Fig. 2), the lowest  
462 correlations between models and observations are found in BA, especially in AMJ for  
463 all models. In particular, EMEP is negatively correlated with observations over this  
464 region. As mentioned above, the larger discrepancies between CTMs and observations  
465 found over BA might be attributed to a low density of observation sites from which the  
466 interpolated dataset is derived, resulting in a lower quality or higher uncertainties of  
467 such product (Schnell et al. 2014). The highest correlations in AMJ are obtained at the  
468 following regions: ME; FR; NI; and EN for most of the models, except for EMEP for  
469 which the highest correlation with observations was found in IN and SC. The WRF-  
470 Chem model also shows a different behaviour in terms of the correlation coefficient  
471 with higher values in NI, MD and IP, and very low and negative correlations (-0.02) in  
472 SC. In general, the models that are most closely correlated with observations are  
473 MATCH, MINNI and CHIMERE, while LOTOS and WRF-Chem show the lowest  
474 correlations. In the case of LOTOS, it could be partially due to the use of a different set-  
475 up of the RACMO2 model, without nudging towards ERA-Interim (section 2.2). These  
476 correlations reflect the patterns represented by the seasonal cycle described above.

477

478 **4.2. MLR performance**

479

480 Figures 4 and 5 depict the statistical performance of each MLR in terms of  $R^2$  and  
481 RMSE (respectively) at the different regions for both seasons, AMJ and JAS. The  $R^2$   
482 values indicate that all MLRs models (based on both observations and CTMs) are able  
483 to explain more than 60% of the MDA8 O<sub>3</sub> variance in all regions. Overall, the MLRs  
484 show a stronger fit in JAS than in AMJ in most of the regions, with the exception of SC  
485 and IN that, in general show lower values of  $R^2$  in JAS than in AMJ (Fig. 4). The MLRs  
486 appear to perform better in certain regions such as NI, ME, FR or EA, while the poorest  
487 statistical performance is found in IN and EN. The results obtained from the CTM-  
488 based MLRs show a similar performance to the observation-based MLRs in most of the  
489 regions. The lowest RMSE values for most of the MLR are found in SC ranging  
490 between 1 and 3 ppb, while EN shows the largest RMSE values, especially for the MLR  
491 built from WRF-Chem (Fig. 5). The MLRs from MATCH and CHIMERE show the  
492 lowest RMSE values (1-3ppb) suggesting the best statistical fit from a predictive point  
493 of view.

494

495 Both  $R^2$  and RMSE metrics indicate that the statistical performance of MLRs for  
496 observations and CTMs show distinct variations between seasons and regions. Overall,



497 better performances are found in JAS and in some regions (i.e. ME, NI, or FR) where  
498 MLRs are able to describe more than the 80% of the variance in CTMs and  
499 observations. This could be attributed to the major role of meteorology in summer  
500 influencing local photochemistry processes of ozone production, while in spring long  
501 range transport plays a stronger role (Monks, 2000, Tarasova et al. 2007). As it includes  
502 the bias, the RMSE reveals more differences among the MLRs when compared to each  
503 other (e.g. larger errors for WRF-Chem or LOTOS when compared to MATCH or  
504 CHIMERE). However, it is interesting that in general all MLRs show a similar  
505 tendency when evaluating the statistical performance, which indicate that observations-  
506 based and CTMs-based MLRs present a similar statistical performance for modelling  
507 MDA8 O<sub>3</sub>. The ability of the CTMs to reproduce the influence of meteorological  
508 drivers on MDA8 O<sub>3</sub> is discussed in more detail below.

509

### 510 4.3. Effects of drivers of ozone concentrations

511

512 The analysis of the influence of the predictors in the MLRs reveals distinctive regional  
513 patterns in both observation-based and CTM-based MLRs. In agreement with Otero et  
514 al. (2016), here we also find that the regions geographically located towards the interior  
515 (including central, western and eastern regions) appear to be more sensitive to the  
516 meteorological predictors, especially in JAS. On the contrary, a minor meteorological  
517 contribution is found in the regions over the northernmost and southernmost edges,  
518 implying that non-local processes play a stronger role. Considering such similarities,  
519 in the following, the regions: EN, FR, ME, NI and EA are referred as the internal regions,  
520 while the rest of the regions: IN, SC, IP, MD and BA, are referred as the external  
521 regions (see Fig. 1).

522

#### 523 4.3.1 Relative importance

524

525 Figure 6 depicts the relative importance of the predictors for the observation-based and  
526 CTM-based MLRs in the internal regions (Fig. 1). Here, a larger meteorological  
527 influence (i.e., the predictors other than LO<sub>3</sub> and day) can be seen in JAS compared to  
528 AMJ in all of these regions. In general, the dominant meteorological drivers from the  
529 observation-based MLRs in these internal regions are RH and Tx. The contribution of  
530 RH is evident in AMJ (e.g. ME, or EA), while Tx is clearly dominant in JAS. SSRD is  
531 also a key driver of MDA8 O<sub>3</sub> and generally, the wind factors (W<sub>10m</sub> and W<sub>dir</sub>)  
532 appear to have a minor contribution.

533

534 Despite the CTM-based MLRs being able to capture the meteorological predictors, we  
535 observe discrepancies among the internal regions when compared to the observation-  
536 based MLR. The inter-model differences in terms of the relative importance of  
537 predictors are greater in AMJ than in JAS. For instance, the contribution of the LO<sub>3</sub> is  
538 overestimated by most of CTMs, specifically WRF-Chem that shows a larger sensitivity  
539 to LO<sub>3</sub> in both seasons over all of these regions. Similarly, EMEP also shows a larger  
540 contribution of LO<sub>3</sub> than the rest of the CTMs, particularly in AMJ. Substantial  
541 differences are found in the influence of RH when comparing the observation-based and  
542 the CTMs-based models. The CTMs do not capture the relative importance of the RH  
543 well, especially in AMJ. In general, the CTMs driven by WRF meteorology show a  
544 slightly larger contribution of RH in most of the cases, although we notice that there are  
545 also some differences among the models that share the same meteorology. CTMs do  
546 capture the relative importance of Tx in all regions, but overall they overestimate it, as



547 they also show for SSRD. Here, we find discrepancies when comparing the contribution  
548 of predictors in the statistical models from CTMs driven by the same meteorology (e.g.  
549 EMEP and WRF-Chem when compared to CHIMERE and MINNI). The largest  
550 differences among the CTMs are found for WRF-Chem, which tends to underestimate  
551 the contribution of the meteorological drivers in most of the regions. Interestingly, as  
552 mentions in Section 2, this is the only online coupled model participating in EDT.

553  
554 Figure 7 presents the relative importance of individual predictors in the MLRs  
555 developed at the external regions (Fig. 1) for both seasons. The observation-based  
556 MLRs show that the main driving factor is LO3 in AMJ, while the effect of  
557 meteorological drivers becomes stronger in JAS. RH presents a larger contribution in  
558 some regions (e.g. IN, IP or SC) in AMJ and Tx in JAS (e.g. IN, IP, SC and BA). The  
559 contribution of wind components, Wdir and W10m, is mainly reflected in both seasons  
560 in the western regions (i.e. IN and IP) and in MD, respectively.

561  
562 Overall, all CTMs show this tendency, although there are substantial differences when  
563 comparing the individual drivers' contribution in the observation-based and CTM-based  
564 MLRs, particularly in AMJ (Fig. 7). CTMs do not capture the contribution of LO3  
565 reflected by the observation-based MLRs. As in the previous analysis (section 4.1) the  
566 largest discrepancies are found in BA, where observation-based MLR shows that most  
567 of the variability of ozone would be explained by LO3. On the contrary the CTM-based  
568 MLRs underestimate the contribution of LO3 and overestimate the meteorological  
569 effect in terms of larger contribution of Tx, SSRD and RH (e.g. LOTOS, CHIMERE  
570 and MINNI). The contribution of RH is underestimated by the CTMs in most of the  
571 regions, (except in BA). On the contrary, the relative importance of SSRD is  
572 overestimated in some regions (e.g. IP, IN or MD) and Tx (IN, SC), in particular for the  
573 CTMs driven by WRF. Overall, CTMs show the observed contribution of W10m and  
574 Wdir in both seasons, although with some inconsistencies among the regions and CTMs.

575  
576 Our results indicate that the relative importance of meteorological factors is stronger in  
577 the internal regions (Fig.6) than in the external regions (Fig.7), which could be partially  
578 attributed to a larger variability of most of the meteorological fields in internal regions  
579 (Fig. S1). The external regions are also more likely to be influenced by the lateral  
580 boundary conditions applied by each CTM. In addition, in some external regions (e.g.  
581 IP or MD), as mentioned in section 2, the use of a coarser grid in some regions might be  
582 insufficient to capture mesoscale processes, such as land-sea breezes, which also control  
583 MDA8 O3 concentrations (Millán et al. 2002). Moreover, we observe that meteorology  
584 becomes more important in summer, when local photochemistry processes are  
585 dominant. In general, CTMs show this tendency, but limitations to reproduce the effect  
586 of some meteorological drivers are found. Specifically, while CTMs tend to  
587 overestimate the contribution of Tx, and SSRD, they underestimate the relative  
588 importance of RH, which is also reflected in the correlations coefficients between  
589 predictand the predictors (Figs. S2, S3).

#### 590 591 4.3.2 Sensitivity of ozone to the drivers

592  
593 We assess the sensitivities of MDA8 O3 to the drivers through their standardised  
594 coefficients obtained in the MLR (Section 3). These coefficients provide further  
595 information about the changes of MDA8 O3 due to effect of each driver. Figures 8 and  
596 9 depict the values of the main driving factors obtained in the MLR for the internal and



597 the external regions (respectively): LO3, Tx and RH. Similarly to those patterns  
598 described by the relative importance of drivers, we observe that the ozone response to  
599 LO3 is stronger in AMJ than in JAS: the corresponding standardised coefficients are  
600 always positive and generally higher in AMJ. The observed sensitivities to LO3 are  
601 smaller in the internal regions (Fig. 8), being particularly dominant in the external  
602 regions (Fig. 9). Overall, most of the CTMs reflect a similar tendency. However, there  
603 are evident differences among observations and CTMs when comparing the values of  
604 the standardised coefficients, specifically in some regions such as BA or MD. When  
605 comparing the ozone responses of the CTMs to LO3, we observe that in most of the  
606 regions MATCH and MINNI show values closest to observations, while WRF-Chem  
607 shows a large sensitivity to LO3.

608  
609 Correlations between MDA8 O3 and Tx are strong, especially in the internal regions in  
610 JAS (Fig. S2). Overall, we show that the CTMs appear to capture the observed effect of  
611 Tx better in JAS than in AMJ in most of the regions. The highest sensitivities to Tx are  
612 found in some internal regions such as ME, NI, FR and EN, which is also shown in the  
613 CTMs. However, we see that most of the CTMs tend to overestimate the effect of Tx.  
614 Moreover, distinct sensitivities to Tx are shown by models that share the same  
615 meteorology (i.e. CHIMERE, EMEP, MINNI and WRF-Chem). In particular, the  
616 MINNI and CHIMERE models show higher Tx sensitivities when compared to the rest  
617 of the CTMs. While MINNI model presents the highest sensitivities to Tx in spring,  
618 specifically in EN and FR, EMEP shows smaller values and it underestimates the  
619 correlations between Tx and MDA8 O3 (Figs. S2, S3).

620  
621 The slope of the ozone-temperature relationship ( $m_{O_3-T}$ ) has been used in several studies  
622 to assess the ozone climate penalty (eg. Bloomer et al., 2009, Steiner et al., 2010,  
623 Rasmussen et al., 2012, Brown-Steiner et al. 2015) in the context of future air quality.  
624 Thus, we additionally analyse the relationship ozone-temperature in order to provide  
625 insight into the ability of CTMs to reproduce the observed  $m_{O_3-T}$ . Similarly as in  
626 previous work (Brown-Steiner et al. 2015), the slopes are obtained from a simple linear  
627 regression using only Tx (without the influence from other predictors) and they are used  
628 to quantify such relationship in both seasons, AMJ and JAS.

629  
630 Figures 10 and 11 illustrate the  $m_{O_3-T}$  for the internal and the external regions  
631 respectively. The observed  $m_{O_3-T}$  is larger in JAS than in AMJ. In AMJ, it ranges  
632 between -0.45 and 1.15 ppbK<sup>-1</sup> with the largest values found in ME, NI and MD. In  
633 JAS, the observed climate penalty is of the order of 1-2.7 ppbK<sup>-1</sup> with the largest values  
634 in EN, FR, ME, NI, and MD. CTMs show a better agreement with observations in JAS  
635 than in AMJ. CTMs tend to overestimate the climate penalty in AMJ in most of the  
636 regions, with some exceptions, such as EMEP and MATCH that systematically  
637 underestimate the slopes. Also, CTMs are generally better in simulating the observed  
638  $m_{O_3-T}$  in the internal regions compared to the  $m_{O_3-T}$  in the external regions, where in  
639 general CTMs appear to overestimate the climate penalty in both seasons. Using this  
640 metric, we identify some regions particularly sensitive to temperature, with larger  
641 values of  $m_{O_3-T}$  (e.g. EN, ME, FR, NI or MD). Through a multi-model assessment,  
642 Colette et al. (2015) showed a significant summertime climate penalty in southern,  
643 western and central European regions (e.g. EA, IP, FR, ME or MD) in the majority of  
644 the future climate scenarios used. Our study shows that most of the CTMs confirm the  
645 observed climate penalty in JAS in such regions in the near present, although we found



646 that most of the CTMs overestimate the climate penalty in AMJ, especially in the  
647 external regions.

648  
649 We see a stronger effect of RH in AMJ than in JAS in the observations compared with  
650 the CTMs (Figs. 8 and 9), with the greatest impact in the internal regions (e.g. EA, ME,  
651 NI, FR and EN). The CTMs show this tendency slightly in some regions (e.g. ME, FR  
652 or EN), but differences become evident when compared to the observed values and  
653 overall they underestimate the effect of RH. As mentioned, CTMs underestimate the  
654 strength of the relationship between ozone-RH (Figs. S2, S3). This general lack of  
655 sensitivity to RH could also partially explain the tendency for all CTMs to show a high  
656 bias in simulated ozone compared with observations (Fig. 2). Among the possible  
657 reasons for this inconsistency, we hypothesize that it can be related to the fact that  
658 ozone removal processes can be associated to higher relative humidity levels during  
659 thunderstorm activity on hot moist days, which might not be well captured by CTMs.  
660 Furthermore, the documented impacts of ozone dry deposition suggest that it may also  
661 play a role in explaining the problems that CTMs show to reproduce the observed  
662 relationship ozone-relative humidity.

663  
664 High SSRD levels favour photochemical ozone formation and it is usually positively  
665 correlated to ozone. In this case, CTMs also present some limitations to capture this  
666 effect and they overestimated the sensitivities of ozone to SSRD (Figs. S4, S5). For  
667 example, the observations show lower and surprisingly negative effect of SSRD.  
668 Although the correlations between SSRD and ozone are positive (see Fig. S2, S3), the  
669 presence of other predictors in the regression may reverse the sign of the estimated  
670 coefficient. The CTMs show a stronger sensitivity of ozone to SSRD and they  
671 overestimate its influence on surface ozone. Similarly, the sensitivities to Wdir and  
672 W10m are also overestimated by the CTMs, especially in AMJ (Figs. S4, S5).

673  
674 Our analysis suggests that CTMs present more limitations to reproduce the influence of  
675 meteorological drivers to MDA8 O<sub>3</sub> concentrations in the external regions than in the  
676 internal regions, particularly in AMJ. Moreover, we find the largest discrepancies in  
677 BA, where models show the poorest seasonal performance and correlation coefficients  
678 (Figs. 2 and 3, respectively), probably due a low quality of the observational dataset.

679  
680 Furthermore, LO<sub>3</sub> is the main driver over most of the external regions and explains a  
681 large proportion to the total variability of MDA8 O<sub>3</sub>, while meteorological factors play  
682 a smaller influence. Lemaire et al. (2016) found a very low performance (based on R<sup>2</sup>)  
683 over the British Isles, Scandinavia and the Mediterranean using a different statistical  
684 approach that only included two meteorological drivers. They attributed this low skill to  
685 the large influence over those regions of long-range transport of air pollution (Lemaire  
686 et al. 2016). Our results confirm the small influence of the meteorological drivers over  
687 those regions and the strong influence of the ozone persistence. Moreover, in the case of  
688 the external regions of northern Europe, it could also be explained due to the dominance  
689 of transport processes such as the stratospheric-tropospheric exchange or long-range  
690 transport from the European continent, rather than local meteorology, particularly in  
691 AMJ (Monks, 2000, Tang et al. 2009, Andersson et al. 2009).

692  
693 Previous work pointed out that local sources of NO<sub>x</sub> and biogenic VOC (ozone  
694 precursors) are important factors of summertime ozone pollution in the Mediterranean  
695 basin (Richards et al. 2013). Moreover, some studies suggested that the local vertical



696 recirculation and accumulation of pollutants play an important role in ozone pollution  
697 episodes in this region: during the nighttime the air masses are held offshore by land-sea  
698 breeze, creating reservoirs of pollutants that are brought the following day (Millán et al.  
699 20002, Jiménez et al. 2006, Querol et al. 2017). All of these factors (e.g. local emissions  
700 as well as local and large-scale processes) control the ozone variability, which might  
701 explain the smaller influence of local meteorological factors shown in this study over  
702 the Mediterranean basin when compared to meteorological influence in the internal  
703 regions. Thus, we may hypothesize that the strong impact of LO<sub>3</sub> observed in the  
704 external regions over southern Europe (i.e. IP, MD, BA) could be partially due to the  
705 role of vertical accumulation and recirculation of air masses along the Mediterranean  
706 coasts as a result of the mesoscale phenomena, which is enhanced by the complex  
707 terrains that surround the Basin. Other important factor for the strong impact of LO<sub>3</sub>  
708 observed is the slow dry deposition of ozone on water that would favour the ozone  
709 persistence in southern Europe.

710  
711 Overall we conclude that CTMs capture the effect of meteorological drivers better in the  
712 internal regions (EN, FR, ME, NI and EA), where the influence of local meteorological  
713 conditions is stronger. The major effect of meteorological parameters found in the  
714 internal European regions might be also attributed to the fact that overall the variability  
715 of meteorological conditions is larger in those regions (Fig. S1). We also find  
716 differences among the CTMs driven by the same meteorology. As mentioned in the  
717 introduction, Bessagnet et al. (2016) suggested that the spread in the model results  
718 could partly explained by the differences in the vertical diffusion coefficient and the  
719 planetary boundary layer, differently diagnosed in each of the CTMs. Our results also  
720 indicate that even though models share the same meteorology (considering the  
721 prescribed requirements defined by the EDT exercise) they show discrepancies when  
722 compared to each other, which could be attributed other sources of uncertainties (such  
723 as physical and chemical internal process in the CTMs). The NMVOC and NO<sub>x</sub>  
724 emissions from the biosphere are critical in the ozone formation. Since biogenic  
725 emissions were not specifically prescribed, which have a strong dependence on  
726 temperature and solar radiation, discrepancies in the CTMs performances, (e.g. different  
727 sensitivities to Tx) might be expected. Furthermore, we notice that the CTMs do not  
728 reproduce consistently the regional ozone-temperature relationship, which is a key  
729 factor when assessing the impacts of climate change on future air quality.

730

## 731 5. Summary and conclusions

732

733 The present study evaluates the capability of a set of Chemical Transport Models  
734 (CTMs) to represent the regional relationship between daily maximum 8-hour average  
735 ozone (MDA8 O<sub>3</sub>) and meteorology over Europe. Our results show systematic  
736 differences between the CTMs in reproducing the seasonal cycle when compared to  
737 observations. In general, they tend to overestimate the MDA8 O<sub>3</sub> in most of the  
738 regions. In the western and northern regions (i.e. Inflow, England and Scandinavia),  
739 some models did not capture the high ozone levels in spring (e.g. CHIMERE, MINNI  
740 and WRF-Chem), while in other southern regions (e.g. Iberian Peninsula,  
741 Mediterranean and Balkans) they overestimated the ozone levels in summer (e.g.  
742 LOTOS, CHIMERE). Of the CTMs, MATCH and MINNI were the most successful in  
743 capturing the observed seasonal cycle of ozone in most regions. All CTMs revealed  
744 limitations to reproduce the variability of ozone over the Balkans region, with a general  
745 overestimation of the ozone concentrations, considerably larger during the warmer



746 months (July, August). As reflected in the results, a limitation of the interpolated  
747 observational product used here is that in some regions (e.g. southern Europe) it has a  
748 lower quality due to a reduced number of stations (section 2.1).

749  
750 The MLRs performed similarly for most of the CTMs and observations, describing  
751 more than 60 % of the total variance of MDA8 O<sub>3</sub>. Overall, the MLRs perform better in  
752 JAS than in AMJ, and the highest percentages of described variance were found in Mid  
753 Europe and North Italy. This could be attributed to local photochemical processes being  
754 more important in JAS, and is consistent with a stronger influence of long-range  
755 transport in AMJ.

756  
757 The effects of predictors revealed spatial and seasonal patterns, in terms of their relative  
758 importance in the MLRs. Particularly, we noticed a larger local meteorological  
759 influence in the regions located towards the interior, here termed as the internal regions  
760 (i.e. England, France, Mid-Europe, North Italy and East-Europe). A minor local  
761 meteorological contribution was found in the rest of the regions, referred as the external  
762 regions (i.e. Inflow, Iberian Peninsula, Scandinavia, Mediterranean and Balkans). The  
763 CTMs are in better agreement with the observations in the internal regions than in the  
764 external regions, where they were not as successful in reproducing the effects of the  
765 ozone drivers. Overall, the different behaviour in the MLRs developed in the external  
766 regions could be attributed to (i) a larger influence of dynamical processes rather than  
767 local meteorological processes (e.g. long range transport in the northern regions) (ii) a  
768 stronger impact of the boundary conditions (iii) the use of a coarser grid that might be  
769 insufficient to capture mesoscale processes that also influence MDA8 O<sub>3</sub> (e.g. sea-land  
770 breezes in the southern regions).

771  
772 We found substantial differences in the sensitivities of MDA8 O<sub>3</sub> to the different  
773 meteorological factors among the CTMs, even when they used the same meteorology.  
774 As Bessagnet et al. (2016) point out, the differences amongst CTMs could be partly  
775 attributed to some other diagnosed model variables (e.g. vertical diffusion coefficient  
776 and boundary layer height, as well as vertical model resolution). To assess the effect of  
777 such potential sources of uncertainties, further investigations would be required.  
778 Moreover, variations in the sensitivity of ozone to meteorological parameters could  
779 depend on differences in the chemical and photolysis mechanisms and the  
780 implementation of various physics schemes, all of which differ between the CTMs (see  
781 Colette et al. 2017a). Specifically, the discrepancies found in the sensitivities of MDA8  
782 O<sub>3</sub> to maximum temperature might be also attributed to biogenic emissions not  
783 prescribed in the models. This was particularly reflected in the analysis of the slopes  
784 ozone-temperature ( $m_{O_3-T}$ ) to assess the climate penalty, which differed between CTMs  
785 and regions when compared to the observations in both seasons. Most of the CTMs  
786 confirm the observed climate penalty in JAS, but with larger discrepancies in the  
787 external regions than in the internal regions. Furthermore, CTMs tend to overestimate  
788 the climate penalty in AMJ (particularly in the external regions).

789  
790 Our results have shown that CTMs tend to overestimate the influence of maximum  
791 temperature and surface solar radiation in most of the regions, both strongly associated  
792 with ozone production. None of the CTMs captured the strength of the observed  
793 relationship between ozone and relative humidity appropriately, underestimating the  
794 effect of relative humidity, a key factor in the ozone removal processes. We speculate  
795 that ozone dry deposition schemes used by the CTMs in this study may not adequately





796 represent the relationship between humidity and stomatal conductance, thus  
797 underestimating the ozone sink due to stomatal uptake. Further sensitivity analyses  
798 would be recommended for testing the impact of the current dry deposition schemes in  
799 the CTMs.

800

#### 801 **Data availability**

802

803 The data are available upon request from the corresponding author.

804

#### 805 **Acknowledgments**

806

807 We acknowledge Jordan L. Schnell for providing the interpolated dataset of MDA 8 O<sub>3</sub>.  
808 Modelling data used in the present analysis were produced in the framework of the  
809 EURODELTA-Trends Project initiated by the Task Force on Measurement and  
810 Modelling of the Convention on Long Range Transboundary Air Pollution.  
811 EURODELTA-Trends is coordinated by INERIS and involves modelling teams of  
812 BSC, CERE, CIEMAT, ENEA, IASS, JRC, MET Norway, TNO, SMHI. The views  
813 expressed in this study are those of the authors and do not necessarily represent the  
814 views of EURODELTA-Trends modelling teams.

815

816

817

818

819

820

821

822

823

824

825

826

827

828

829

830

831

832

833

834

835

836

837

838

839

840

841

842

843

844

845

846 **List of Tables:**

847

CTM	Meteorology	Coupling
LOTOS-EUROS	RACMO2	Off-line
MATCH	HIRLAM	Off-line
EMEP	WRF	Off-line
CHIMERE		Off-line
MINNI		Off-line
WRF-Chem		On-line

848

849

850

851

852

**Table 1.** List of the chemistry-transport models used in the study, their corresponding meteorological driver and chemistry/meteorology coupling.

Predictor	Definition	853
LO3	Lag of O <sub>3</sub> (24 h)	854
Tx	Maximum temperature	855
RH	Relative humidity	856
SSRD	Surface solar radiation	857
Wdir	Wind direction	858
W10m	Wind speed	859
day	$\sin(2\pi d/365.25)$ ,	860
	$\cos(2\pi d/365.25)$	861
		862

863

864

865

866

**Table 2.** List of the predictors used in the multiple linear regression analysis: meteorological parameters, lag of O<sub>3</sub> (24h, previous day) and the seasonal cycle components.

Region	Acronym	Coordinates (longitude, latitude)	867
England	EN	5W-2E, 50N-55N	868
Inflow	IN	10W-5W, 50N-60N, and 5W-2E, 55N-60N	869
Iberian Peninsula	IP	10W-3E, 36N-44N	870
France	FR	5W-5E, 44N-50N	871
Mid-Europe	ME	2E-16E, 48N-55N	872
Scandinavia	SC	5E-16E, 55N-70N	873
North Italy	NI	5E-16E, 44N-48N	874
Balkans	BA	18E-28E, 38N-44N	875
Mediterranean	MD	3E-18E, 36N-44N	876
Eastern Europe	EA	16E-30E, 44N-55N	877
			878
			879
			880
			881

882

883

884

885

886

887

888

889

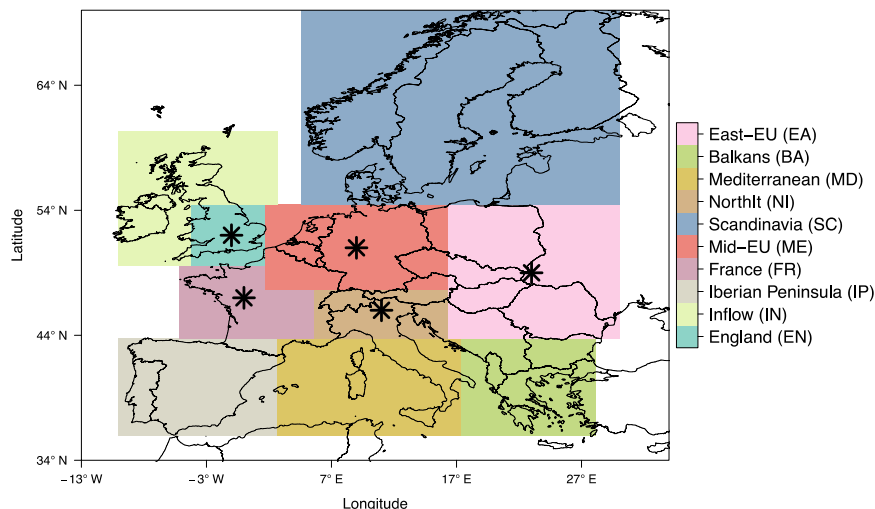
890

891

**Table 3.** List of the regions with the short name and the coordinates.

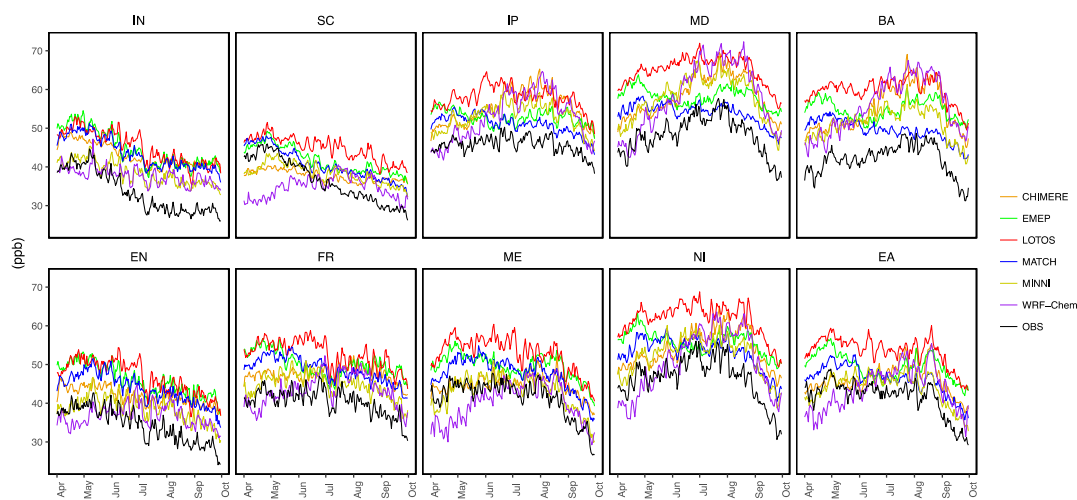


892 **List of Figures:**  
893  
894  
895



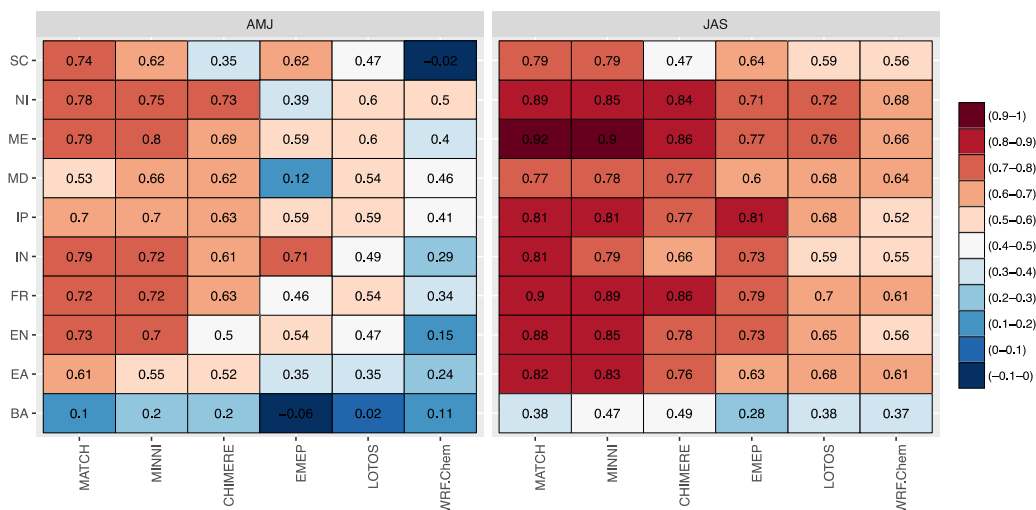
896  
897  
898  
899  
900  
901

**Figure 1.** Map of the regions considered in the study. Regions indicated with a black star are referred to the internal regions in the text. The rest of regions are referred to the external regions of the European domain.



902  
903  
904  
905  
906  
907

**Figure 2.** Time series of daily averages of MDA8 O<sub>3</sub> during the ozone season (April-September) for the period of study (2000-2010) at each subregion.



908

909

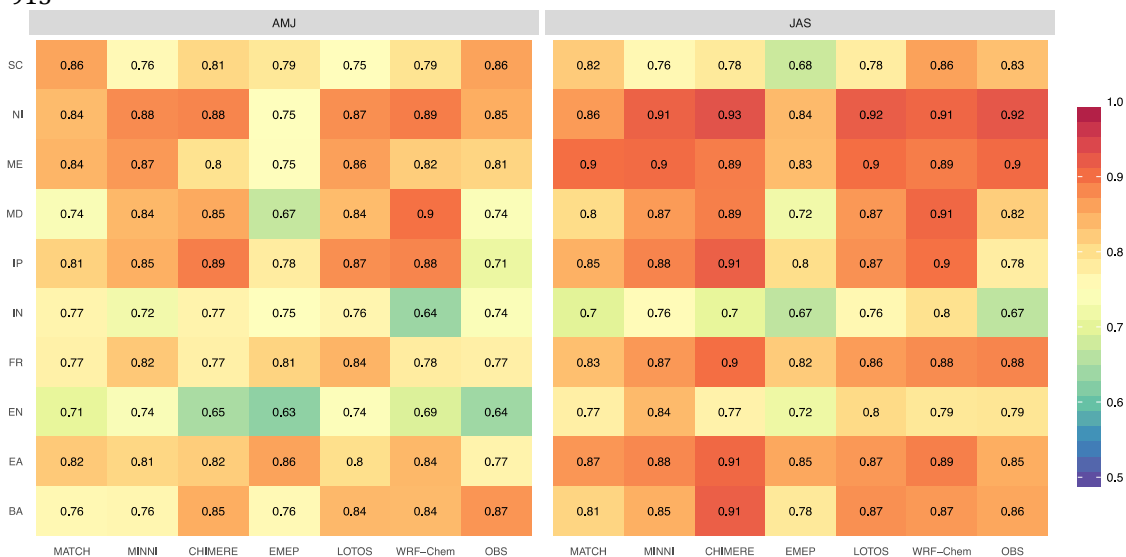
910

911

912

913

**Figure 3.** Correlation coefficients between observed and modelled MDA8 O3 for spring (AMJ) and summer (JAS) for the period of study (2000-2010) at each region (rows) and models (columns, ordered by highest correlation values).



914

915

916

917

918

919

920

921

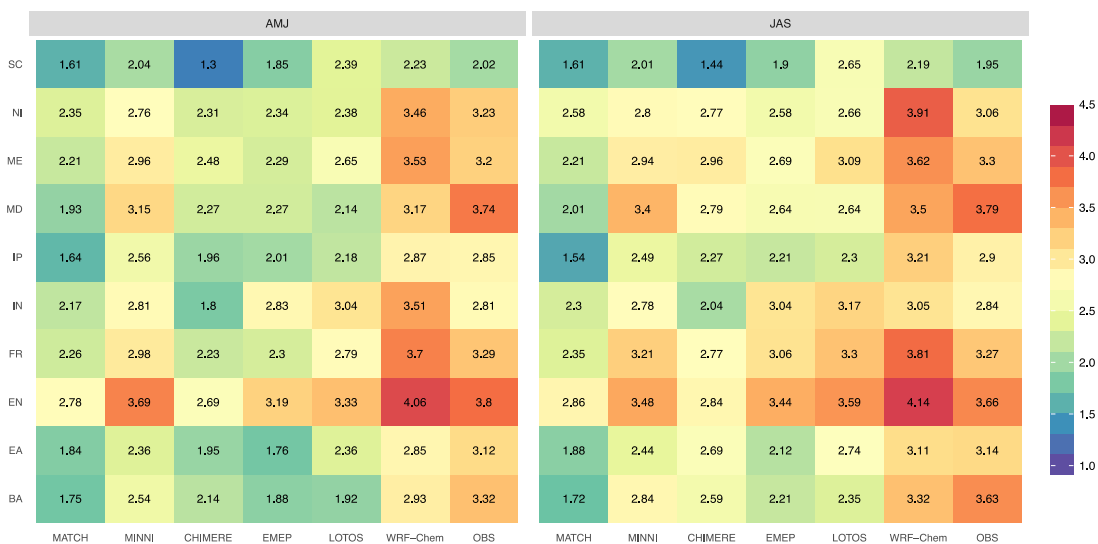
922

923

**Figure 4.** Coefficients of determination ( $R^2$ ) for each CTM-based (ordered as in Fig.3) and observation-based MLR in spring (AMJ) and summer (JAS).

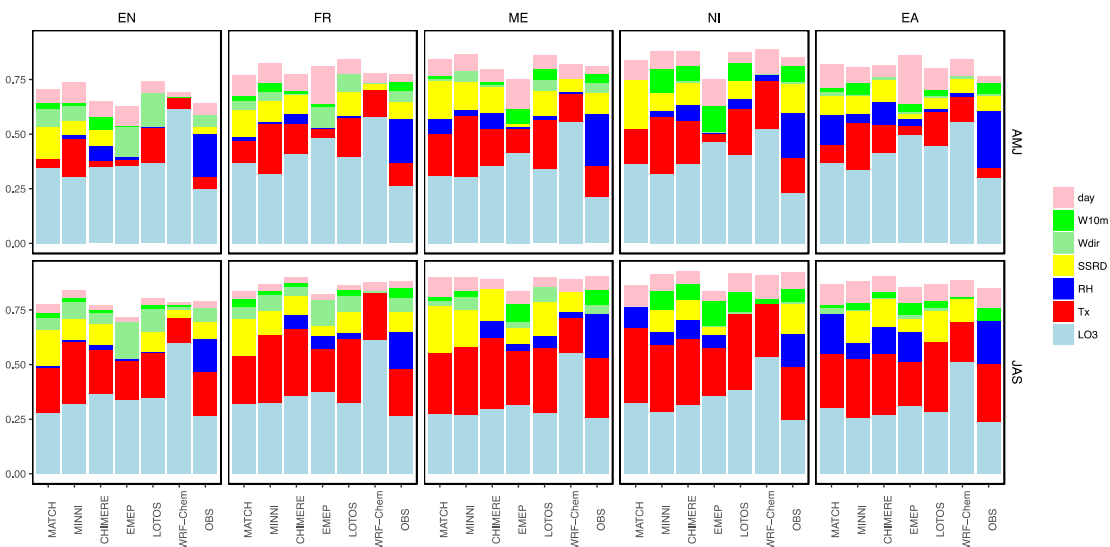


924



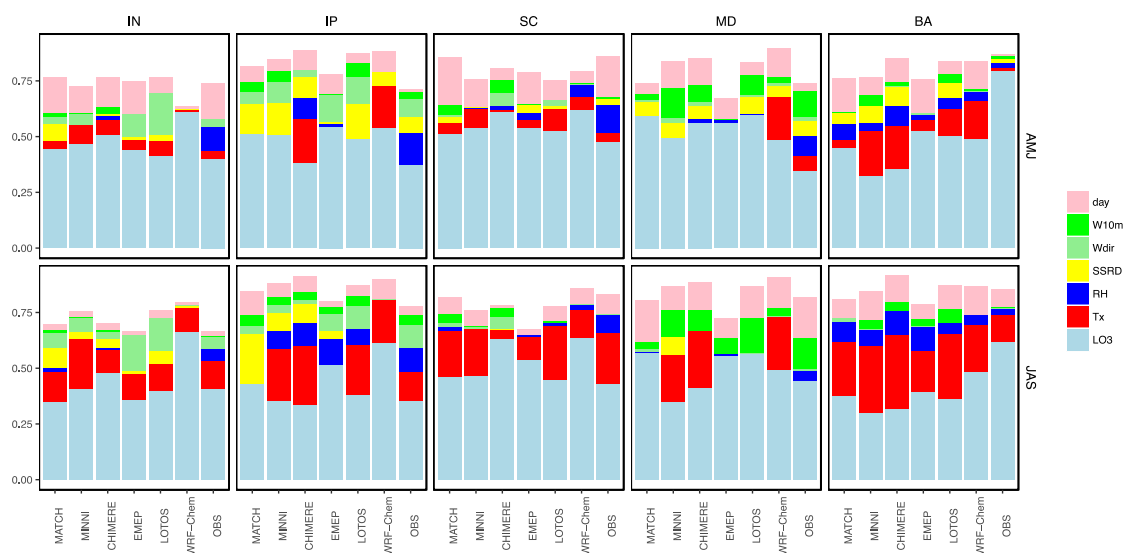
925  
 926  
 927  
 928  
 929  
 930  
 931

**Figure 5.** Root mean square errors (RMSE) for each CTM-based (ordered as in Fig.3) and observation-based MLR at each region, in spring (AMJ) and summer (JAS).

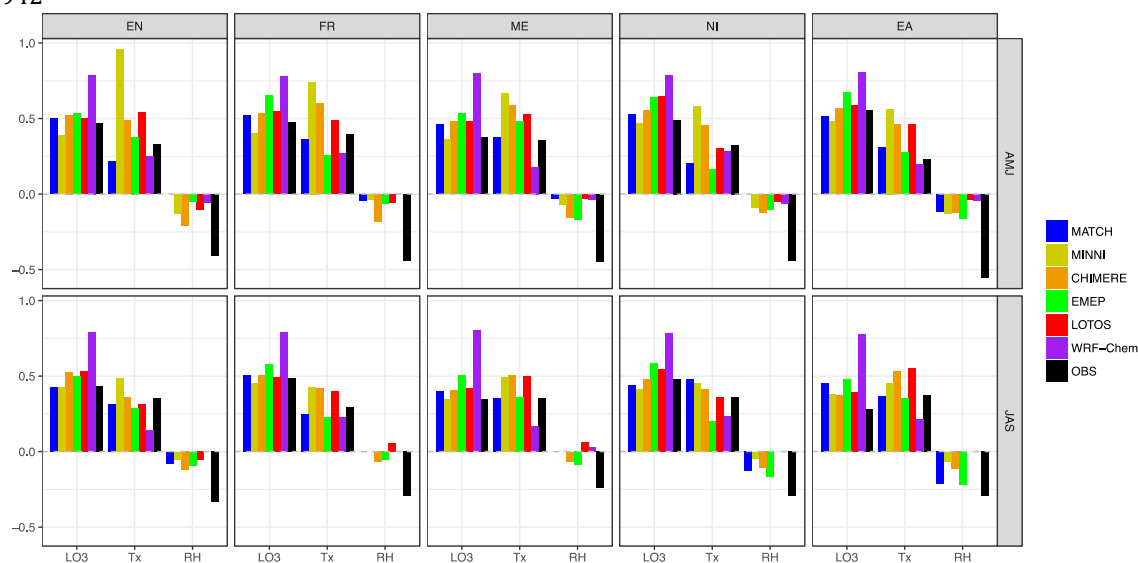


932  
 933  
 934  
 935  
 936

**Figure 6.** Proportion of each predictor to the total explained variance for each CTM-based (ordered as in Fig.3) and observation-based MLR in AMJ (top) and JAS (bottom) for the internal regions: England (EN), France (FR), Mid-Europe (ME), North Italy (NI) and East-Europe (EA).



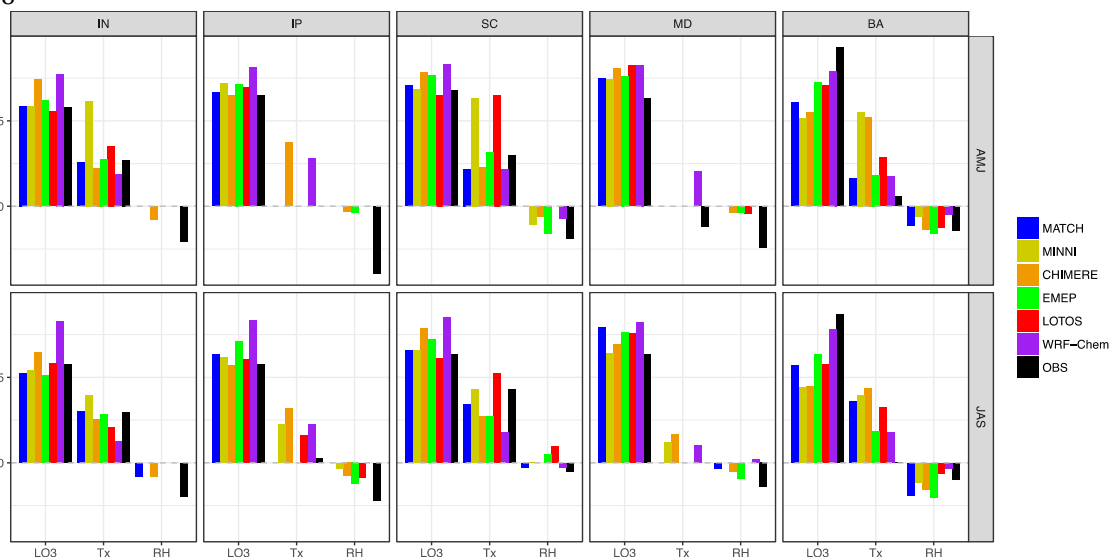
937  
938 **Figure 7.** Proportion of each predictor to the total explained variance for each CTM-based (ordered as in  
939 Fig.3) and observation-based MLR in AMJ (top) and JAS (bottom) for the external regions: Inflow (IN),  
940 Iberian Peninsula (IP), Scandinavia (SC), Mediterranean (ME) and Balkans (BA).  
941  
942



943  
944 **Figure 8.** Standardised coefficients values of the main key-driving factors (LO3, Tx and RH) for each  
945 CTM-based (ordered as in Fig.3) and observation-based MLR in AMJ (top) and JAS (bottom) and for the  
946 internal regions: England (EN), France (FR), Mid-Europe (ME), North Italy (NI) and East-Europe (EA).  
947

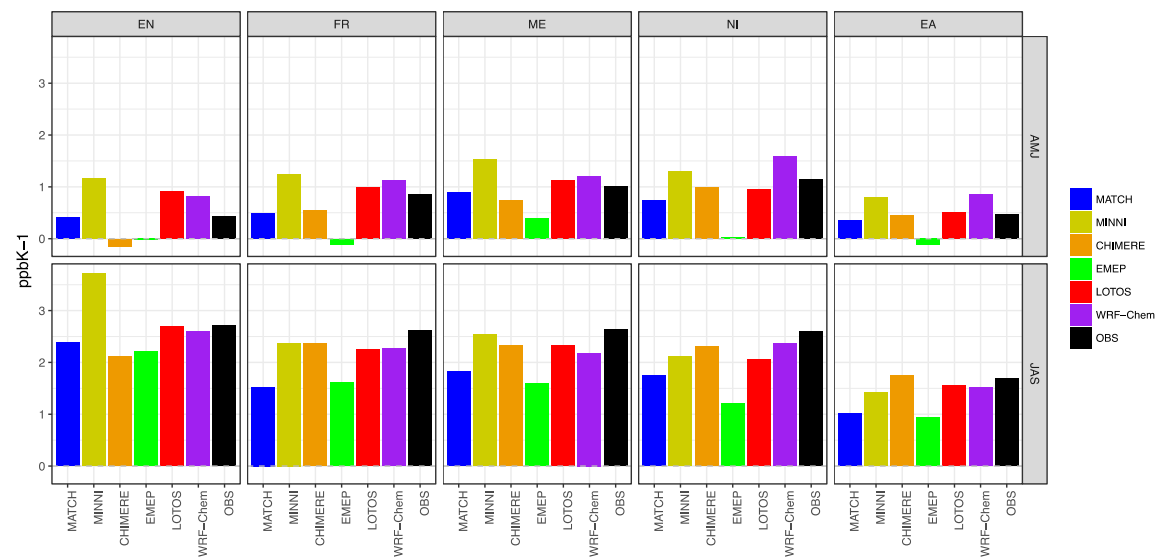


948



949

950 **Figure 9.** Standardised coefficients values of the main key-driving factors (LO3, Tx and RH) for each  
 951 CTM-based (ordered as in Fig.3) and observation-based MLR in AMJ (top) and JAS (bottom) and for the  
 952 external regions: Inflow (IN), Iberian Peninsula (IP), Scandinavia (SC), Mediterranean (ME) and Balkans  
 953 (BA).



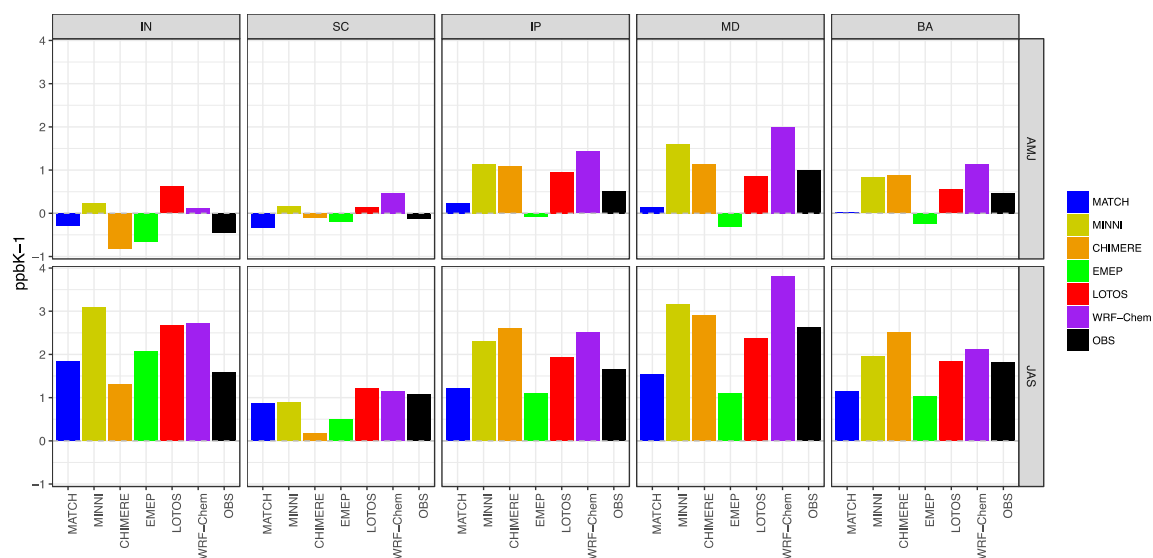
954

955

956 **Figure 10.** Slopes ( $m_{O_3-T}$ ; ppbK<sup>-1</sup>) obtained from a simple linear regression to estimate the relationship  
 957 ozone-temperature for each CTM-based (ordered as in Fig.3) and observation-based MLR in AMJ (top)  
 958 and JAS (bottom) and for the internal regions: England (EN), France (FR), Mid-EU (ME), North Italy  
 959 (NI), East-EU (EA).

960

961



962

963

964 **Figure 11.** Slopes ( $m_{O_3-T}$ ;  $ppbK^{-1}$ ) obtained from a simple linear regression to estimate the relationship

965 ozone-temperature for each CTM-based (ordered as in Fig.3) and observation-based MLR in AMJ (top)

966 and JAS (bottom) and for the external regions: Inflow (IN), Iberian Peninsula (IP), Scandinavia (SC),

967 Mediterranean (ME) and Balkans (BA).

967





968

969

**References**

970

971 Andersson, C., J. Langner, and R. Bergström: Interannual variation and trends in air  
972 pollution over Europe due to climate variability during 1958–2001 simulated with a  
973 regional CTM coupled to the ERA-40 reanalysis, *Tellus, Ser. B*, 59, 77–98, 2007.

974

975 Andersson C., Bergström R., Johansson C., Population exposure and mortality due to  
976 regional background PM in Europe—Long-term simulations of source region and  
977 shipping contributions, *Atmospheric Environment*, 43, 22, 3614–3620,  
978 <http://dx.doi.org/10.1016/j.atmosenv.2009.03.040>, 2009.

979

980 Andersson, C. and Engardt, M.: European ozone in a future climate: Importance of  
981 changes in dry deposition and isoprene emissions, *J. Geophys. Res.-Atmos.*, 115,  
982 D02303, doi:10.1029/2008jd011690, 2010.

983

984 Baklanov, A., Schlünzen, K., Suppan, P., Baldasano, J., Brunner, D., Aksoyoglu, S.,  
985 Carmichael, G., Douros, J., Flemming, J., Forkel, R., Galmarini, S., Gauss, M., Grell,  
986 G., Hirtl, M., Joffre, S., Jorba, O., Kaas, E., Kaasik, M., Kallos, G., Kong, X.,  
987 Korsholm, U., Kurganskiy, A., Kushta, J., Lohmann, U., Mahura, A., Manders-Groot,  
988 A., Maurizi, A., Moussiopoulos, N., Rao, S. T., Savage, N., Seigneur, C., Sokhi, R. S.,  
989 Solazzo, E., Solomos, S., Sørensen, B., Tsegas, G., Vignati, E., Vogel, B., and Zhang,  
990 Y.: Online coupled regional meteorology chemistry models in Europe: current status  
991 and prospects, *Atmos. Chem. Phys.*, 14, 317–398, doi:10.5194/acp-14-317-2014, 2014.

992

993 Barrero M A, Grimalt J O and Canton L.: Prediction of daily ozone concentration  
994 maxima in the urban atmosphere *Chemometr. Intell. Lab. Syst.* 80 67–76, 2005.

995

996 Bessagnet, B., Pirovano, G., Mircea, M., Cuvelier, C., Aulinger, A., Calori, G., Ciarelli,  
997 G., Manders, A., Stern, R., Tsyro, S., García Vivanco, M., Thunis, P., Pay, M.-T.,  
998 Colette, A., Couvidat, F., Meleux, F., Rouil, L., Ung, A., Aksoyoglu, S., Baldasano, J.  
999 M., Bieser, J., Briganti, G., Cappelletti, A., D'Isidoro, M., Finessi, S., Kranenburg, R.,  
1000 Silibello, C., Carnevale, C., Aas, W., Dupont, J.-C., Fagerli, H., Gonzalez, L., Menut,  
1001 L., Prévôt, A. S. H., Roberts, P., and White, L.: Presentation of the EURODELTA III  
1002 intercomparison exercise – evaluation of the chemistry transport models' performance  
1003 on criteria pollutants and joint analysis with meteorology, *Atmos. Chem. Phys.*, 16,  
1004 12667–12701, doi:10.5194/acp-16-12667-2016, 2016.

1005

1006 Bloomfield P J, Royle J A, Steinberg L J and Yang Q: Accounting for meteorological  
1007 effects in measuring urban ozone levels and trends *Atmos. Environ.* 30 3067–77, 1996 .

1008

1009 Bloomer, B. J., Stehr, J. W., Piety, C. A., Salawitch, R. J., and Dickerson, R. R.:  
1010 Observed relationships of ozone air pollution with temperature and emissions, *Geophys.*  
1011 *Res. Lett.*, 36, L09803, doi:10.1029/2009gl037308, 2009.

1012

1013 Brown-Steiner, B., Hess, P. G., and Lin, M. Y.: On the capabilities and limitations of  
1014 GCM simulations of summertime regional air quality: A diagnostic analysis of ozone  
1015 and temperature simulations in the US using CESM CAM-Chem, *Atmos. Environ.*, 101,  
1016 134–148, doi:10.1016/j.atmosenv.2014.11.001, 2015.

1017



- 1018 Camalier, L., Cox, W., and Dolwick, P.: The effects of meteorology on ozone in urban  
1019 areas and their use in assessing ozone trends, *Atmos. Environ.*, 41, 7127–7137, 2007.  
1020
- 1021 Chaloulakou A, Saisana M and Spyrellis N: Comparative assessment of neural networks  
1022 and regression models for forecasting summertime ozone in Athens *Science of the Total*  
1023 *Environment* 313 1–13, 2003.  
1024
- 1025 Coates, J., Mar, K. A., Ojha, N., and Butler, T. M.: The influence of temperature on  
1026 ozone production under varying NO<sub>x</sub> conditions – a modelling study, *Atmos. Chem.*  
1027 *Phys.*, 16, 11601–11615, <https://doi.org/10.5194/acp-16-11601-2016>, 2016.  
1028
- 1029 Colette, A., Andersson, C., Baklanov, A., Bessagnet, B., Brandt, J., Christensen, J.,  
1030 Doherty, R., Engardt, M., Geels, C., Giannakopoulos, C., Hedegaard, G., Katragkou, E.,  
1031 Langner, J., Lei, H., Manders, A., Melas, D., Meleux, F., Rouil, L., Sofiev, M., Soares,  
1032 J., Stevenson, D., Tombrou-Tzella, M., Varotsos, K., and Young, P.: Is the ozone  
1033 climate penalty robust in Europe?, *Environ. Res. Lett.*, 10, 084015, doi:10.1088/1748-  
1034 9326/10/8/084015, 2015.  
1035
- 1036 Colette, A., Andersson, C., Manders, A., Mar, K., Mircea, M., Pay, M.-T., Raffort, V.,  
1037 Tsyro, S., Cuvelier, C., Adani, M., Bessagnet, B., Bergström, R., Briganti, G., Butler,  
1038 T., Cappelletti, A., Couvidat, F., D'Isidoro, M., Doumbia, T., Fagerli, H., Granier, C.,  
1039 Heyes, C., Klimont, Z., Ojha, N., Otero, N., Schaap, M., Sindelarova, K., Stegehuis, A.  
1040 I., Roustan, Y., Vautard, R., van Meijgaard, E., Vivanco, M. G., and Wind, P.:  
1041 EURODELTA-Trends, a multi-model experiment of air quality hindcast in Europe over  
1042 1990–2010, *Geosci. Model Dev. Discuss.*, <https://doi.org/10.5194/gmd-2016-309>,  
1043 accepted, 2017a.  
1044
- 1045 Colette, A., Solberg, S., Beauchamp, M., Bessagnet, B., Malherbe, L., and Guerreiro,  
1046 C.: Long term air quality trends in Europe: Contribution of meteorological variability,  
1047 natural factors and emissions, ETC/ACM, Bilthoven, 2017b.  
1048
- 1049 Comrie A. C. : Comparing neural networks and regression models for ozone forecasting  
1050 *J. Air Waste Manage. Assoc.* 47 653–63, 1997.  
1051
- 1052 Dahlgren, P., Landelius, T., Kållberg, P., and Gollvik, S.: A high-resolution regional  
1053 reanalysis for Europe. Part 1: Three-dimensional reanalysis with the regional High-  
1054 Resolution Limited-Area Model (HIRLAM), *Quarterly Journal of the Royal*  
1055 *Meteorological Society*, 142, 2119–2131, 10.1002/qj.2807, 2016.  
1056
- 1057 Davis, J., Cox, W., Reff, A., Dolwick, P.: A comparison of Cmaq-based and  
1058 observation-based statistical models relating ozone to meteorological parameters.  
1059 *Atmospheric Environment* 45, 3481e3487. [http://dx.doi.org/10.1016/](http://dx.doi.org/10.1016/J.Atmosenv.2010.12.060)  
1060 *J.Atmosenv.2010.12.060*, 2011.
- 1061 Dawson, J.P., Adams, P.J., Pandis, S.N.: Sensitivity of ozone to summertime climate in  
1062 the Eastern USA: a modeling case study. *Atmos. Environ.* 41, 1494– 1511, 2007.  
1063
- 1064 Dawson, J. P., Racherla, P. N., Lynn, B. H., Adams, P. J., and Pan- dis, S. N.:  
1065 Simulating present-day and future air quality as cli- mate changes: model evaluation,  
1066 *Atmos. Environ.*, 42, 4551– 4566, doi:10.1016/j.atmosenv.2008.01.058, 2008.



- 1067  
1068 Dee D P et al. :The ERA-Interim reanalysis: configuration and performance of the data  
1069 assimilation system *Quart. J. R. Meteorol. Soc.* 137 553–97, 2001.  
1070  
1071 Doherty, R. M., Wild, O., Shindell, D. T., Zeng, G., MacKenzie, I. A., Collins, W. J.,  
1072 Fiore, A. M., Stevenson, D. S., Dentener, F. J., Schultz, M. G., Hess, P., Derwent, R.  
1073 G., and Keating, T. J.: Impacts of climate change on surface ozone and intercontinental  
1074 ozone pollution: a multi- model study, *J. Geophys. Res.-Atmos.*, 118, 3744–3763,  
1075 doi:10.1002/jgrd.50266, 2013.  
1076  
1077 Elminir H.K.: Dependence of urban air pollutants on meteorology, *Science of The Total*  
1078 *Environment*, 350,225-237, <http://dx.doi.org/10.1016/j.scitotenv.2005.01.043>, 2005.  
1079  
1080 Fischer M., Rust H.W., and Ulbrich U.: Seasonality in extreme precipitation – using  
1081 extreme value statistics to describe the annual cycle in german daily precipitation.  
1082 *Meteorol. Z.* accepted, 2017.  
1083  
1084 Fiore, A. M., Dentener, F. J., Wild, O., Cuvelier, C., Schultz, M. G., Hess, P., Textor,  
1085 C., Schulz, M., Doherty, R. M., Horowitz, L. W., MacKenzie, I. A., Sanderson, M. G.,  
1086 Shindell, D. T., Stevenson, D. S., Szopa, S., Van Dingenen, R., Zeng, G., Atherton, C.,  
1087 Bergmann, D., Bey, I., Carmichael, G., Collins, W. J., Duncan, B. N., Faluvegi, G.,  
1088 Folberth, G., Gauss, M., Gong, S., Hauglustaine, D., Holloway, T., Isaksen, I. S. A.,  
1089 Jacob, D. J., Jonson, J. E., Kaminski, J. W., Keating, T. J., Lupu, A., Marmer, E.,  
1090 Montanaro, V., Park, R. J., Pitari, G., Pringle, K. J., Pyle, J. A., Schroeder, S., Vivanco,  
1091 M. G., Wind, P., Wojcik, G., Wu, S., and Zuber, A.: Multimodel estimates of  
1092 intercontinental source-receptor relationships for ozone pollution, *J. Geophys. Res.-*  
1093 *Atmos.*, 114, D04301, doi:10.1029/2008jd010816, 2009.  
1094  
1095 Gan C., Hogrefe C., Mathur R., Pleim J., Xing J., Wong D., Gilliam R., Pouliot G., Wei  
1096 C.: Assessment of the effects of horizontal grid resolution on long-term air quality  
1097 trends using coupled WRF-CMAQ simulations, *Atmospheric Environment*, 132, 207-  
1098 216,1352-2310,<https://doi.org/10.1016/j.atmosenv.2016.02.036>, 2016.  
1099  
1100 Grell, G. A., Peckham, S. E., Schmitz, R., McKeen, S. A., Frost, G., Skamarock, W. C.,  
1101 and Eder, B.: Fully coupled “online” chemistry within the WRF model, *Atmospheric*  
1102 *Environment*, 39, 6957-6975, <http://dx.doi.org/10.1016/j.atmosenv.2005.04.027>, 2005.  
1103  
1104 Grömping U. : Estimators of relative importance in linear regression based on variance  
1105 decomposition *Am. Stat.* 61 139–47, 2007.  
1106  
1107 Hedegaard, G. B., Christensen, J. H., and Brandt, J.: The relative importance of impacts  
1108 from climate change vs. emissions change on air pollution levels in the 21st century,  
1109 *Atmos. Chem. Phys.*, 13, 3569-3585, doi:10.5194/acp-13-3569-2013, 2013.  
  
1110 Hendriks C., Forsell N., Kiesewetter G., Schaap M., Schöpp W.: Ozone concentrations  
1111 and damage for realistic future European climate and air quality scenarios, *Atmospheric*  
1112 *Environment*, 144, 208-219, <http://dx.doi.org/10.1016/j.atmosenv.2016.08.026>, 2016.  
1113  
1114 Hodnebrog, Ø., Solberg, S., Stordal, F., Svendby, T. M., Simpson, D., Gauss, M.,  
1115 Hilboll, A., Pfister, G. G., Turquety, S., Richter, A., Burrows, J. P., and Denier van der



- 1116 Gon, H. A. C.: Impact of forest fires, biogenic emissions and high temperatures on the  
1117 elevated Eastern Mediterranean ozone levels during the hot summer of 2007, *Atmos.*  
1118 *Chem. Phys.*, 12, 8727–8750, <https://doi.org/10.5194/acp-12-8727-2012>, 2012  
1119
- 1120 Hogrefe, C., Biswas, J., Lynn, B., Civerolo, K., Ku, J. Y., Rosenthal, J., Rosenzweig,  
1121 C., Goldberg, R., and Kinney, P. L.: Simulating regional-scale ozone climatology over  
1122 the eastern United States: model evaluation results, *Atmos. Environ.*, 38, 2627–2638,  
1123 2004.  
1124
- 1125 IPCC, *Climate Change 2013, the Physical Science Basis. Working Group I contribution*  
1126 *to the fifth assessment report of the Intergovernmental Panel on Climate*  
1127 *Change*, Cambridge University Press, 2013.  
1128
- 1129 Jacob, D. J. and Winner, D. A.: Effect of climate change on air quality, *Atmos.*  
1130 *Environ.*, 43, 51–63, doi:10.1016/j.atmosenv.2008.09.051, 2009.  
1131
- 1132 Jonson, J. E., Simpson, D., Fagerli, H., and Solberg, S.: Can we explain the trends in  
1133 European ozone levels?, *Atmos. Chem. Phys.*, 6, 51–66, doi:10.5194/acp-6-51-2006,  
1134 2006.
- 1135 Kavassalis, S. C., and J. G. Murphy: Understanding ozone-meteorology correlations: A  
1136 role for dry deposition, *Geophys. Res. Lett.*, 44, 2922–2931,  
1137 doi:10.1002/2016GL071791, 2017.  
1138
- 1139 Kong, X., Forkel R., Sokhi R. S., Suppan P., Baklanov A., Gauss M., Brunner D., Barò  
1140 R., Balzarini A., Chemel C., Curci G., Jiménez-Guerrero P., Hirtl M., Honzak L., Im U.,  
1141 Pérez J. L., Pirovano G., San Jose R., Schlünzen K. H., Tsegas G., Tuccella P.,  
1142 Werhahn J., Žabkar R., Galmarini S.: Analysis of Meteorology-Chemistry Interactions  
1143 During Air Pollution Episodes Using Online Coupled Models within AQMEII Phase-2,  
1144 *Atmospheric Environment*, <http://dx.doi.org/10.1016/j.atmosenv.2014.09.020>, 2014.  
1145
- 1146 Kutner M. H., Nachtsheim C. J. and Neter J.: *Applied Linear Regression Models 4th Ed*  
1147 (Boston, MA: McGraw-Hill Irwin) 2004.  
1148
- 1149 Langner, J., Bergström R. and Foltescu V.: Impact of climate change on surface ozone  
1150 and deposition of sulphur and nitrogen in Europe, *Atmos. Environ.*, 39, 1129–1141,  
1151 doi:10.1016/j.atmosenv.2004.09.082, 2005.  
1152
- 1153 Lelieveld, J., and P. J. Crutzen: Influence of cloud and photochemical processes on  
1154 tropospheric ozone, *Nature*, 343, 227–233, 1990.
- 1155 Lemaire, V. E. P., Colette, A. and Menut, L.: Using statistical models to explore  
1156 ensemble uncertainty in climate impact studies: the example of air pollution in Europe,  
1157 *Atmos. Chem. Phys.*, 16, 2559–2574, doi:10.5194/acp-16-2559-2016, 2016.  
1158
- 1159 Lindeman R.H., Merenda P. F. and Gold RZ: *Introduction to Bivariate and Multivariate*  
1160 *Analysis*. Scott, Foresman, Glenview, IL, 1980.  
1161
- 1162 Linderson M. L.: Objective classification of atmospheric circulation over southern  
1163 Scandinavia *Int. J. Climatol.* 21 155–69, 2001.



- 1164  
1165 Mailler, S., Menut, L., Khvorostyanov, D., Valari, M., Couvidat, F., Siour, G.,  
1166 Turquety, S., Briant, R., Tuccella, P., Bessagnet, B., Colette, A., Létinois, L., Markakis,  
1167 K., and Meleux, F.: CHIMERE-2017: from urban to hemispheric chemistry-transport  
1168 modeling, *Geosci. Model Dev.*, 10, 2397-2423, [https://doi.org/10.5194/gmd-10-2397-](https://doi.org/10.5194/gmd-10-2397-2017)  
1169 2017, 2017.
- 1170 Maindonald J, Braun J: Data analysis and graphics using R: an example-based  
1171 approach. Cambridge (United Kingdom), Cambridge University Press, 2006.  
1172
- 1173 Manders, A. M. M., van Meijgaard, E., Mues, A. C., Kranenburg, R., van Ulft, L. H.,  
1174 and Schaap, M.: The impact of differences in large-scale circulation output from climate  
1175 models on the regional modeling of ozone and PM, *Atmos. Chem. Phys.*, 12, 9441–  
1176 9458, doi:10.5194/acp-12-9441-2012, 2012.  
1177
- 1178 Manders, A. M. M., Bultjes, P. J. H., Curier, L., Denier van der Gon, H. A.  
1179 C., Hendriks, C., Jonkers, S., Kranenburg, R., Kuenen, J., Segers, A. J.,  
1180 Timmermans, R. M. A., Visschedijk, A., Wichink Kruit, R. J., Van Pul, W. A. J.,  
1181 Sauter, F. J., van der Swaluw, E., Swart, D. P. J., Douros, J., Eskes, H., van  
1182 Meijgaard, E., van Ulft, B., van Velthoven, P., Banzhaf, S., Mues, A., Stern, R.,  
1183 Fu, G., Lu, S., Heemink, A., van Velzen, N., and Schaap, M.: Curriculum Vitae of  
1184 the LOTOS-EUROS (v2.0) chemistry transport model, *Geosci. Model Dev. Discuss.*,  
1185 <https://doi.org/10.5194/gmd-2017-88>, in review, 2017.  
1186
- 1187 Mar, K. A., Ojha, N., Pozzer, A. and Butler, T. M.: Ozone air quality simulations with  
1188 WRF-Chem (v3.5.1) over Europe: model evaluation and chemical mechanism  
1189 comparison, *Geosci. Model Dev.*, 9, 3699- 3728, [10.5194/gmd-9-3699-2016](https://doi.org/10.5194/gmd-9-3699-2016), 2016.  
1190
- 1191 Meijgaard, E. v., van Ulft, L. H., Lenderink, G., de Roode, S. R., Wipfler, L., Boers, R.,  
1192 and Timmermans, R. M. A.: Refinement and application of a regional atmospheric  
1193 model for climate scenario calculations of Western Europe, *KvR 054/12*, 44, 2012.  
1194
- 1195 Meleux, F., Solmon, F., and Giorgi, F.: Increase in summer European ozone amounts  
1196 due to climate change, *Atmos. Environ.*, 41, 7577–7587,  
1197 doi:10.1016/j.atmosenv.2007.05.048, 2007.  
1198
- 1199 Millán, M. M., Sanz, M. J., Salvador, R., and Mantilla, E.: Atmospheric dynamics and  
1200 ozone cycles related to nitrogen deposition in the western Mediterranean, *Environ.*  
1201 *Pollut.*, 118, 167–186, 2002.  
1202
- 1203 Mills, G., Hayes, F., Jones, M. L. M., and Cinderby, S.: Identifying ozone-sensitive  
1204 communities of (semi-)natural vegetation suitable for mapping exceedance of critical  
1205 levels, *Environ. Pollut.*, 146, 736–743, doi:10.1016/j.envpol.2006.04.005, 2007.  
1206
- 1207 Mircea, M., Grigoras, G., D’Isidoro, M., Righini, G., Adani, M., Briganti, G.,  
1208 Ciancarella, L., Cappelletti, A., Calori, G., Cionni, I., Cremona, G., Finardi, S., Larsen,  
1209 B. R., Pace, G., Perrino, C., Piersanti, A., Silibello, C., Vitali, L., and Zanini, G.: Impact  
1210 of grid resolution on aerosol predictions: a case study over Italy, *Aerosol and Air*  
1211 *Quality Research*, 1253–1267, doi: 10.4209/aaqr.2015.02.0058, 2016.  
1212



- 1213 Monks, P. S.: A review of the observations and origins of the spring ozone maximum,  
1214 Atmos. Environ., 34, 3545–3561, 2000.  
1215
- 1216 Monks, P. S., Archibald, A. T., Colette, A., Cooper, O., Coyle, M., Derwent, R.,  
1217 Fowler, D., Granier, C., Law, K. S., Mills, G. E., Stevenson, D. S., Tarasova, O.,  
1218 Thouret, V., von Schneidemesser, E., Sommariva, R., Wild, O., and Williams, M. L.:  
1219 Tropospheric ozone and its precursors from the urban to the global scale from air  
1220 quality to short-lived climate forcer, Atmos. Chem. Phys., 15, 8889–8973,  
1221 <https://doi.org/10.5194/acp-15-8889-2015>, 2015.  
1222
- 1223 Ordóñez, C., Mathis, H., Furger, M., Henne, S., Hoglin, C., Staehelin, J., Prevot,  
1224 A.S.H.: Changes of daily surface ozone maxima in Switzerland in all seasons from 1992  
1225 to 2002 and discussion of summer 2003. Atmos. Chem. Phys. 5, 1187– 1203, 2005.  
1226
- 1227 Porter W C, Heald C L, Cooley D and Russell B 2015 Investigating the observed  
1228 sensitivities of air quality extremes to meteorological drivers via quantile regression  
1229 Atmos. Chem. Phys. Discuss. 15 10349–66, 2015.  
1230
- 1231 Pusede S E et al. : On the temperature dependence of organic reactivity, nitrogen  
1232 oxides, ozone production, and the impact of emission controls in San Joaquin Valley,  
1233 California Atmos. Chem. Phys. 14 3373–95, 2014.  
1234
- 1235 Querol, X., Gangoiti, G., Mantilla, E., Alastuey, A., Minguillón, M. C., Amato, F.,  
1236 Reche, C., Viana, M., Moreno, T., Karanasiou, A., Rivas, I., Pérez, N., Ripoll, A.,  
1237 Brines, M., Ealo, M., Pandolfi, M., Lee, H.-K., Eun, H.-R., Park, Y.-H., Escudero, M.,  
1238 Beddows, D., Harrison, R. M., Bertrand, A., Marchand, N., Lyasota, A., Codina, B.,  
1239 Olid, M., Udina, M., Jiménez-Esteve, B., Soler, M. R., Alonso, L., Millán, M., and Ahn,  
1240 K.-H.: Phenomenology of high-ozone episodes in NE Spain, Atmos. Chem. Phys., 17,  
1241 2817–2838, <https://doi.org/10.5194/acp-17-2817-2017>, 2017.  
1242
- 1243 Rasmussen, D. J., Fiore, A. M., Naik, V., Horowitz, L. W., McGinnis, S. J., and  
1244 Schultz, M. G.: Surface ozone-temperature relationships in the eastern US: A monthly  
1245 climatology for evaluating chemistry-climate models, Atmos. Environ., 47, 142–153,  
1246 doi:10.1016/j.atmosenv.2011.11.021, 2012.  
1247
- 1248 Robertson, L., Langner, J., and Engardt, M.: An Eulerian Limited-Area Atmospheric  
1249 Transport Model, Journal of Applied Meteorology, 38, 190–210, 1999.  
1250
- 1251 Rust H, Maraun D. and Osborn T.: Modelling seasonality in extreme precipitation Eur.  
1252 Phys. J. Special Topics 174 99–111, 2009.  
1253
- 1254 Rust H. W., Vrac M., Sultan B., and Lengaigne M.: Mapping weather-type influence on  
1255 Senegal precipitation based on a spatial-temporal statistical model. J. Climate, 26:8189–  
1256 8209. ISSN 0894-8755. URL <http://dx.doi.org/10.1175/JCLI-D-12-00302.1.1>. 2013  
1257
- 1258 Schaap, M., Timmermans, R. M. A., Roemer, M., Boersen, G. A. C., Bultjes, P.,  
1259 Sauter, F., Velders, G., and Beck, J.: The LOTOS-EUROS model: description,  
1260 validation and latest developments, International Journal of Environment and Pollution,  
1261 32, 270–290, 2008.  
1262



- 1263 Schaap M., Cuvelier C., Hendriks C., Bessagnet B., Baldasano J.M., Colette A., Thunis  
1264 P., Karam D., Fagerli H., Graff A., Kranenburg R., Nyiri A., Pay M.T., Rouil L., Schulz  
1265 M., Simpson D., Stern R., Terrenoire E., Wind P.: Performance of European chemistry  
1266 transport models as function of horizontal resolution, *Atmospheric Environment*, 112,  
1267 90-105, <http://dx.doi.org/10.1016/j.atmosenv.2015.04.003>, 2015.
- 1268  
1269 Skamarock, W. C., Klemp, J. B., Dudhia, J., Gill, D. O., Barker, D. M., Duda, M. G.,  
1270 Huang, X. Y., Wang, W., and Powers, J. G.: A Description of the Advanced Research  
1271 WRF Version 3, NCAR, 2008.
- 1272  
1273 Schnell, J. L., Holmes, C. D., Jangam, A., and Prather, M. J.: Skill in forecasting  
1274 extreme ozone pollution episodes with a global atmospheric chemistry model, *Atmos.*  
1275 *Chem. Phys.*, 14, 7721–7739, doi:10.5194/acp-14-7721-2014, 2014.
- 1276  
1277 Schnell, J. L., Prather, M. J., Josse, B., Naik, V., Horowitz, L. W., Cameron-Smith, P.,  
1278 Bergmann, D., Zeng, G., Plummer, D. A., Sudo, K., Nagashima, T., Shindell, D. T.,  
1279 Faluvegi, G., and Strode, S. A.: Use of North American and European air quality  
1280 networks to evaluate global chemistry–climate modeling of surface ozone, *Atmos.*  
1281 *Chem. Phys.*, 15, 10581-10596, doi:10.5194/acp-15-10581-2015, 2015.
- 1282  
1283 Seo, J., Youn, D., Kim, J. Y., and Lee, H.: Extensive spatiotemporal analyses of surface  
1284 ozone and related meteorological variables in South Korea for the period 1999–2010,  
1285 *Atmos. Chem. Phys.*, 14, 6395-6415, <https://doi.org/10.5194/acp-14-6395-2014>, 2014.
- 1286  
1287 Sillman, S. and Samson, P.J: Impact of temperature on oxidant photochemistry in  
1288 urban, polluted rural and remote environments. *Journal of Geophysical Research* 100:  
1289 doi: 10.1029/94JD02146. issn: 0148-0227, 1995.
- 1290  
1291 Solberg, S., R. G. Derwent, Ø. Hov, J. Langner, and A. Lindskog: European abatement  
1292 of surface ozone in a global perspective, *Ambio*, 34, 47–53, 2005.
- 1293  
1294 Solberg, S., Hov, Ø., Sovde, A., Isaksen, I. S. A., Coddeville, P., De Backer, H.,  
1295 Forster, C., Orsolini, Y., and Uhse, K.: European surface ozone in the extreme summer  
1296 2003, *J. Geophys. Res. Atmos.*, 113, D07307, doi:10.1029/2007jd009098, 2008.
- 1297  
1298 Solberg, S., Colette, A., and Guerreiro, C. B. B.: Discounting the impact of meteorology  
1299 to the ozone concentration trends. ETC/ACM, NILU, INERIS.  
1300 <https://doi.org/10.13140/rg.2.2.15389.92649>, 2016.
- 1301  
1302 Steiner, A.L., Tonse, S., Cohen, R.C., Goldstein, A.H., Harley, R.A.: Influence of  
1303 future climate and emissions on Regional air quality in California. *Journal of*  
1304 *Geophysical Research-Atmospheres* 111, 2006.
- 1305  
1306 Vautard, R., Honore, C., Beekmann, M., and Rouil, L.: Simulation of ozone  
1307 during the August 2003 heat wave and emission control scenarios, *Atmos.*  
1308 *Environ.*, 39, 2957–2967, doi:10.1016/j.atmosenv.2005.01.039, 2005.
- 1309  
1310 Tang L., Chen D.L., Karlsson P.E., Gu Y.F., Ou T.H. Synoptic circulation and its  
1311 influence on spring and summer surface ozone concentrations in Southern Sweden  
1312 *Boreal Environment Research*, 14, 889-902, 2009.



- 1313  
1314 Tarasova, O. A., Brenninkmeijer, C. A. M., Jöckel, P., Zvyagintsev, A. M., and  
1315 Kuznetsov, G. I.: A climatology of surface ozone in the extra tropics: cluster analysis of  
1316 observations and model results, *Atmos. Chem. Phys.*, 7, 6099–6117, doi:10.5194/acp-7-  
1317 6099-2007, 2007.  
1318  
1319 Thompson M L, Reynolds J, Cox L H, Guttorp P and Sampson P D: A review of  
1320 statistical methods for the meteorological adjustment of tropospheric ozone *Atmos.*  
1321 *Environ.* 35 617–30, 2001.  
1322  
1323 van Loon, M., Vautard, R., Schaap, M., Bergström, R., Bessagnet, B., Brandt, J.,  
1324 Builtjes, P. J. H., Christensen, J. H., Cuvelier, C., Graff, A., Jonson, J. E., Krol, M.,  
1325 Langner, J., Roberts, P., Rouil, L., Stern, R., Tarrasón, L., Thunis, P., Vignati, E.,  
1326 White, L., and Wind, P.: Evaluation of long-term ozone simulations from seven regional  
1327 air quality models and their ensemble, *Atmospheric Environment*, 41, 2083-2097, 2007.  
1328  
1329 Wu, S., Mickley, L. J., Leibensperger, E. M., Jacob, D. J., Rind, D., and Streets, D. G.:  
1330 Effects of 2000–2050 global change on ozone air quality in the United States, *J.*  
1331 *Geophys. Res.-Atmos.*, 113, D18312, doi:10.1029/2007JD009639, 2008.  
1332  
1333 Zhang, Y.: Online-coupled meteorology and chemistry models: his- tory, current status,  
1334 and outlook, *Atmos. Chem. Phys.*, 8, 2895– 2932, doi:10.5194/acp-8-2895-2008, 2008.  
1335